Viscoelastic Characterization and Effective Damping of a Carbon/Polyurethane Laminate

Niren Pallegonde Kumar
np1860@rit.edu

Rochester Institute of Technology

Viscoelastic Characterization and Effective Damping of a Carbon/Polyurethane Laminate

By

Niren Pallegonde Kumar

A Thesis Submitted
In
Partial Fulfillment of the
Requirements for the Degree in
Master of Science
In
Mechanical Engineering
Supervised by

Dr. Hany Ghoneim

Department of Mechanical Engineering
Kate Gleason College of Engineering
Rochester Institute of Technology
Rochester, New York

May 2016

The thesis "Viscoelastic Characterization and Effective Damping of a Carbon/Polyurethane Laminate" by Niren Pallegonde Kumar has been examined and approved by the following Examination Committee:

Dr. Hany Ghoneim
Professor
Dept. of Mechanical Engineering

_ _
(Thesis Committee Chair)

Dr. Benjamin Varela
Associate Professor
Dept. of Mechanical Engineering

_ _
(Committee Member)

Dr. Kathleen Lamkin Kennard
Associate Professor
Dept. of Mechanical Engineering

_ _
(Committee Member)

Dr. Agamemnon Crassidis
Associate Professor
Director Mechanical Engineering
Dept. of Mechanical Engineering

_ _
(Department Representative)

Dedication

To my dear parents, Dr. P.R. Kumar and Mrs. Shoba Kumar

Acknowledgements

First I would like to express my deepest appreciation to my advisor, Dr. Hany Ghoneim. I am very grateful that Dr. Ghoneim gave me this opportunity to work with him. I really appreciate his patience and guidance during the course of this research and inspiring me to get into this field. He has provided vital insight into the world of composites and vibrations engineering as well as general advice in completing this thesis. A special thanks also goes to Dr. Benjamin Varela and Mr. Tom Allston (Dept. of Chemistry, College of Science) without whom my experimental analysis would not have been possible.

I would also like to thank Dr. Benjamin Varela, Dr. Kathleen Lamkin Kennard and Dr. Agamemnon Crassidis for taking time to review and assist with my work.

I am also thankful for the help provided by Mr. Rob Kraynik and Mr. Jan Maneti in the machine shop, and Ms. Stephanie Webster (Writing Commons, Wallace Center) to help put this document together.

I would like to thank my parents for their support on my graduate study. I would like to acknowledge Mr. Prithviraj Shelke and Ms. Kathleen Ellis and the entire Geo-Polymer Lab for their help and providing me with constant motivational support throughout the course of this research. I also need to thank Ms. Swathi Adisheshu, Vindhya.K.M and all my childhood friends back home for their help and constant encouragement.

Abstract

Two very important factors in determining the effectiveness of a pump are its volumetric and energy efficiencies. Yin and Ghoneim constructed a prototype of a flexible body pump with a high volumetric efficiency (pumping potential). The high volumetric efficiency was attributed to the geometry of the pump's structure (hyperboloid) as well as the high negative effective Poisson's ratio of the 3-layer ($[\theta/\beta/\theta]$) flexible matrix composite (Carbon/Polyurethane) laminate adopted for the body of the pump. The energy efficiency was not evaluated. An important factor in assessing the energy efficiency is the effective damping (energy dissipation) of the flexible body material. The objective of the current research is to evaluate the viscoelastic material properties (Analytically & Experimentally) and the effective damping of the 3-layer ($[\theta/\beta/\theta]$) Carbon/Polyurethane laminate as a function of the two angle orientations θ and β. Consequently, identify the fiber angle orientation for the best volumetric and energy efficiencies of the flexible body pump.

Table of Contents

List of Figures

List of Tables

Nomenclature

ASME	-	American Society of Mechanical Engineers
ν	-	Poisson's Ratio
η	-	Damping Factor
$\sigma(t)$, $\varepsilon(t)$	-	Stress and strain at time 't'
σ_0, ε_0	-	Maximum Stress and Strain
w	-	Frequency of Oscillation
E', E''	-	Storage and Loss Modulus
$\tan\delta$	-	Damping in the matrix
α_T	-	Temperature Shift Factor
C_1, C_2	-	WLF Constants
V_f, V_m	-	Fiber and Matrix Volume Fraction
W_f, W_m	-	Fiber and Matrix Weight Fraction
E_1, E_2	-	Extensional Longitudinal and Transverse modulus
G_{12}	-	In-Plane Shear Modulus
ν_{12}	-	In-Plane Poisson's Ratio
σ_4, σ_5	-	Inter-Laminar Stresses
$\varepsilon_1, \varepsilon_2, \gamma_{12}$	-	In-Plane Strains
$\sigma_1, \sigma_2, \tau_{12}$	-	In-Plane Stresses
G_{23}	-	Out of Plane Shear Modulus
k	-	Lamina number
N_x, N_y, N_{xy}	-	Tensile and Shear forces per unit length along the laminate
M_x, M_y, M_{xy}	-	Moments per unit length along the laminate
θ, β	-	Fiber angle orientation
E_x, E_y	-	Extensional laminate modulus in X and y direction.
G_{xy}	-	Laminate shear modulus
E_b	-	Laminate bending modulus

Chapter 1

Introduction

Viscoelasticity is the property of materials that exhibits both viscous and elastic characteristics when undergoing deformation. When an elastic material undergoes deformation due to an external force, it experiences internal forces (or stress) that oppose the deformation and restore it to its original state after the external forces are removed. However, for viscous materials on the other hand, when stress is removed part of the energy is not returned back to the forcing agent but rather is dissipated with respect to time. The behavior of elastic materials are time/rate independent, whereas the behavior of viscoelastic materials are time/rate dependent. Figure.1 shows the schematic representation of the stress strain diagram for both elastic and viscoelastic materials. Purely elastic materials do not dissipate energy when a load is applied and then removed (Fig 1a); Purely viscous materials dissipate all the energy when a load is applied and then removed (Fig 1b); however viscoelastic materials partially dissipate energy when a load is applied and removed (Fig 1c), i.e., hysteresis is observed in the stress strain curve, with the area enclosed by the loop being equal to the amount of energy lost during the cycle.

Figure.1: Schematic representation of the stress-strain diagrams for elastic and viscoelastic materials (a) Elastic materials (b) Viscous materials (c) Viscoelastic materials

1.1. Damping and Dynamic Behavior

Damping is defined as the decrease in the amplitude of oscillation (free vibration) as a result of energy being drained from the system. Damping can be achieved by active or passive means, or a combination of both. Active damping mechanisms in general add weight and complexity but provide good damping results. On the other hand, passive damping mechanisms increase the reliability and also reduce the complexity of the system and can be achieved by structural modifications and using damping materials.

Viscoelasticity of a material can be best studied using Dynamic Mechanical Analysis, i.e., by applying small oscillatory stress and measuring the resulting strain (which will be further explained in the literature review). For purely elastic materials the stress and strain vectors are in phase, whereas for viscous materials there is a phase lag of 90 degrees (i.e. output strain lags input stress). Viscoelastic materials, on the other hand, exhibit behavior somewhere in between these two materials, i.e. exhibiting some lag in strain.

1.2. Vibration Isolators

Viscoelastic materials are well adapted to be used as vibration isolators because they dissipate part of the energy absorbed as heat. The most effective way to reduce unwanted vibration is to stop or modify the source of the vibration. If this cannot be done, it is sometimes possible to design a vibration isolation system to isolate the source of vibration from the system of interest or to isolate the device from the source of vibration. Most polymers are viscoelastic and are also used as vibration isolators. Certain polymer materials can be manufactured with a wide range of properties such as high damping and strength over a useful range of temperatures and frequencies, but most of these materials lack sufficient rigidity and good creep resistance (ability to resist deformation under prolonged loads). To make up for these deficiencies, polymer materials can be reinforced to produce a composite material [1].

1.3. Composite Materials

A composite material is formed by the combination of two or more chemically distinct materials to obtain a new material with enhanced properties. The characteristics of the composites are completely different from the individual constituents used. Most composite materials consist of two distinct phases i.e. the primary phase and the secondary phase. The primary phase forms the matrix within which the secondary phase is embedded, and the secondary phase is the embedded phase, also known as the reinforcing agent. Based on the type of reinforcements used, the composites can be classified as fiber reinforced composites or particle reinforced composites. For our research we use fiber reinforced composites because particles and flakes are not as effective as using fibers since the composites are usually much stronger and stiffer in this form.

1.3.1. Fibers

Fibers provide most of the stiffness and strength, i.e. they enhance the mechanical and physical properties of the composites. The fiber materials are classified in two ways: continuous fibers (Fig. 2.a) and discontinuous fibers (Fig. 2.b). The most commonly used fibers are glass fibers, silicon fibers and carbon fibers. For our current research work we use carbon fibers. Carbon fibers, also called graphite fibers, are lightweight and strong with excellent chemical resistance. They have a high specific modulus and specific strength. The mechanical properties of carbon fibers are determined by the atomic configuration of carbon chains and their connections, which are similar to the graphite crystal structure. The strength of carbon fiber is controlled by orienting the carbon atomic structures with their strongest atomic connections along the carbon fiber direction. Unlike glass fibers, carbon fibers are available with a broad range of stiffness values. In a carbon fiber, the layers of carbon are oriented along the fiber axis, thus making the mechanical properties stronger along the axial direction.

(a)   (b)

Figure.2: Fiber classification (a) Continuous fibers (b) Discontinuous fibers

1.3.2. Matrix

The matrix has many functions: it holds the fibers together, thus transferring the load through the interface to the reinforcing fibers. Some properties of the composites such as transverse stiffness and strength are matrix dominated. The matrix also plays a leading role in heat and electrical conductivity of the composite. The matrix materials can be polymers, metals or ceramics. Polymer matrices are the most common because of their ease of fabrication, light weight, low tooling cost, low capital investment and low manufacturing costs. The polymer matrices are classified into thermosets, thermoplastics and elastomers. For our current research work we use Polyurethane (PU) as the matrix material.

Polyurethane is an ideal example of an elastomer. Elastomers generally have low modulus, high strength, superior tear strength and abrasion resistance and good low temperature impact properties. They are commonly used in automobile bumpers and flexible composite applications.

1.3.3. Laminates

A unidirectional lamina (ply) is made up of a set of fibers oriented in a single direction within the matrix. Laminates (Fig.3) are made by stacking many unidirectional laminae at different fiber orientation angles. The properties of a composite as a whole change with fiber orientation angle, thickness and stacking order of individual laminas.

Figure.3: Schematic representation of laminate

1.3.4. Flexible Matrix Composites (FMC)

The Flexible Matrix Composites (FMC) are a branch of composite materials wherein strong and stiff reinforcements are combined with elastomeric polymer matrix materials such as polyurethanes, silicones, natural rubbers, etc. Flexible Matrix Composites (FMC) when manufactured along with continuous fibers can withstand large strains in the transverse direction plus retain their strength and stiffness in the fiber direction. The elastic properties of FMCs can be tailored over a much broader range than that offered by the conventional rigid matrix composites (RMCs). FMC have found a wide range of applications including flexible body pump and vibration isolation mounts. The diaphragm pumps, the jellyfish inspired flexible pump [2] and the left ventricle pump [3] are examples of compliant body pumps. The tunable fluidic composite mounts [4] and the controllable suspension system invented by Carlson et al, [5] are examples of FMC in vibration isolation mounts.

1.4. Objective of Proposed Work

There are two research objectives in this study:

1. To determine the viscoelastic characteristics (longitudinal, transverse and shear complex moduli, as well as the complex in-plane Poisson's ratio) of a polyurethane/carbon composite.

2. Provide a detailed study on the effect of the two fiber orientation angles θ and β on the effective damping factors of a three-layer laminate [$\theta/\beta/\theta$] as shown in Figure 4.

Figure.4: A schematic representation of a 3-layer laminate to be investigated.

Using this research coupled with a similar study on the negative Poisson's ratio [6], in general the best fiber orientation angle (θ and β) for structural applications (pumps, suspensions etc.) can be defined, more specifically the fiber orientation of a novel pump proposed by Dr. Ghoneim can be suggested.

Chapter 2

Viscoelasticity and Literature Review

This chapter gives us an insight into the basic analytical techniques and experimental work used to determine the viscoelastic properties and effective damping of a Carbon/Polyurethane laminate. For all standard linear viscoelastic solids, the harmonically varying stress and strain relations are given by [7],

$$\epsilon(t) = \epsilon_0 e^{i\omega t} = \epsilon_0[cos(wt) + isin(wt)] \tag{1}$$

$$\sigma(t) = \sigma_0 e^{i\omega t} = \sigma_0[cos(wt) + isin(wt)] \tag{2}$$

where $\sigma(t)$ is the stress at time (t), $\epsilon(t)$ is the strain at any time (t), σ_0 is the amplitude of the stress, ϵ_0 is the strain amplitude, ω is the frequency of oscillation and t is the time [7]. As per the standard linear model or the Zener Model [8], the relationship between stress σ and strain ε is given by,

$$\sigma(t) + a\frac{d\sigma(t)}{dt} = E\epsilon(t) + bE\frac{d\epsilon(t)}{dt} \tag{3}$$

where, 'a' is the retardation time and 'b' is the creep relaxation time.

From Eqns 1-3, we get the stress-strain relationship in the frequency domain to be,

$$\sigma_0 = E\epsilon_0\frac{1 + i\omega b}{1 + i\omega a} = (E' + iE'')\epsilon_0 \tag{4}$$

where, E' and E'' are the storage and loss moduli, respectively:

The Storage Modulus (E') represents the stiffness of a viscoelastic material and is proportional to the energy stored during a loading cycle. It is an in-phase component,

$$E' = Re\frac{1 + i\omega b}{1 + i\omega a}E \tag{5}$$

The Loss Modulus (E'') is the measure of viscous response of the material. It is also called the imaginary modulus or out of phase component,

$$E'' = Img\frac{1 + i\omega b}{1 + i\omega a}E \tag{6}$$

It should also be mentioned that, the damping factor (tanδ) is also introduced as a measure of damping. It is a dimensionless property, which represents the ratio of loss modulus over the storage modulus.

$$Tan(\delta) = \frac{E''}{E'} \tag{7}$$

In equations [3-7], E stands for the extensional or shear modulus depending on the type of loading applied.

2.1. Experimental Determination of the Viscoelastic Properties of Polymers

Viscoelastic properties of polymers are best determined using the Dynamic Mechanical Analysis (DMA), where a small oscillatory stress is applied and the resulting strain is measures [7].

2.1.1 Dynamic Mechanical Analysis

The Dynamic Mechanical Analysis (DMA) is a widely accepted research technique in the polymer industry, measuring modulus and damping over a wide range of temperatures and frequencies and providing important information about the cure of thermoset resins and aging of thermoplastics [7]. A typical example of a Dynamic Mechanical Analyzer (Perkins Elmer DMA 8000) is shown in Figure. 5. This technique can be expanded to investigate damping properties of composite materials [9]. The method provides fast and reliable results using very small amount of material, which can in many cases be taken directly from the part, in addition to precise temperature and atmosphere control [8].

Figure.5: The Perkins Elmer DMA 8000 [11].

The DMA's usually have built-in functions to directly evaluate viscoelastic properties. The DMA measured properties can be used along with the time-temperature superposition to predict the long term behavior of the material [10]. Frequency scans are the most commonly used technique to study the material behavior in DMA; however, the frequency scan is an ill-defined technique associated with a predictive method called Time-Temperature Superposition. To collect frequency data, the simplest approach is to hold the temperature constant and scan several frequencies while scanning the temperature [9]. The DMA works by applying a sinusoidal deformation to a sample of known geometry. The sample can be subjected by a controlled stress or a controlled strain. For a known stress, the sample will then deform a certain amount. In the DMA this is done sinusoidally. How much it deforms is related to its stiffness. A drive motor is used to generate the sinusoidal wave and this is transmitted to the sample via a drive shaft [9]. A schematic representation of the DMA used is shown in Figure. 6.

Figure.6: A schematic representation of a DMA (Perkins Elmer DMA 8000) [11].

2.1.2. Time Temperature Superposition

The Time Temperature Superposition (TTS) principle makes it possible to characterize the viscoelastic properties of materials at various temperatures over the range of experimentally convenient frequencies [23]. The curve shifting procedure creates a master curve that represents frequency response of a material over a wide range of temperatures, and frequencies at a selected reference temperature [10]. Based on this principle, plots of the material properties vs frequency at various temperatures can be collapsed onto one master curve, with the use of the appropriate Temperature Shift Factor (α_T) [13].

The application of the principle involves the following steps:-

1. Experimental determination of frequency dependent curves of isothermal viscoelastic mechanical properties at several temperatures and for a small frequency range.
2. Computation of the Shift Factor to correlate these properties for the temperature and frequency range.
3. Use of the Shift Factor to determine the master curve showing the effect of frequency for a wider range of frequencies at a reference temperature.

2.1.3. Shift Factor (α_T)

The WLF Equation was coined by William-Landel-Ferry and is used to represent the temperature shifting function [13]. It is often calculated using an empirical relation which is given by,

$$Log(\alpha_t) = \frac{-C_1(T - T_0)}{C_2 + (T - T_0)}$$

(8)

where C_1 and C_2 are the WLF constants to be determined experimentally, T_0 is the reference temperature on which the master curve is created and α_T is the temperature shift factor. This equation is proven useful for a broad range of viscoelastic materials. A typical representation of the data collected using a DMA-8000 at various temperatures within a limited range of

frequencies is shown in Figure.7 [14]. A graph representing a typical master curve created after the TTS is applied to the data obtained from the DMA-8000 is as shown in Figure. 8.

Figure.7: Typical representation of data from the DMA [14].

Figure.8: A typical representation of a master curve [14].

2.1.4. Temperature Dependence of Viscoelastic Behavior

The temperature dependence has two primary points of interest. Firstly, from a single experimental technique (at a given temperature), it is impossible to obtain a complete range of measuring frequencies to evaluate the relaxation spectrum. Therefore as a matter of convenience we change the temperature of the experiment to bring the relaxation process of interest within a time-scale that is readily available. Secondly, polymers change from glass-like to rubber-like behavior as either the temperature is increased or the frequency of the experiment is decreased.

According to J.D.D Melo and Donald W. Radford [13] the viscoelastic properties of PEEK/IM7 were determined over a temperature range of -20 C to +120 C. The storage modulus and loss factor (tan δ) data, from two specimens of PEEK/IM7 tested for different fiber orientation angles, and the corresponding curve fits are presented in Figures 9-11. It was found that for all unidirectional laminae there was an increase in tan δ (Damping) and slight decrease in dynamic

moduli (Storage or Loss Moduli) with increasing temperature. However the temperature influence was different between unidirectional laminae specimens with different fiber orientations. It is understood that in specimens where the properties are more fiber dominated, the temperature effect is reduced [13].

Figure.9: Temperature data for unidirectional lamina with fibers oriented at 0' [13].

Figure.10. Temperature data for unidirectional lamina with fibers oriented at 30' [13].

Figure.11: Temperature data for unidirectional lamina with fibers oriented at 90' [13].

2.1.5. Frequency Dependence of Viscoelastic Behavior

According to Alexander RASA [24] the Dynamic Mechanical Analysis (DMA) is used as a method to investigate and characterize the damping properties of viscoelastic materials. A variety of polymer based materials were tested for their damping properties. The DMA was able to return precise results. The DMA can also be useful for quality assurance because of its ability to identify minor variations in the material composition and processing [24]. According to A. Katunin and W. Hufenbach [25] the influence of temperature and frequency on the loss rigidity for linearly viscoelastic laminate was determined. The DMA experiments conducted showed good agreement of measurements with the theoretical models [25]. In a study conducted by J.D.D. Melo and Donald W. Radford [13], the frequency effects on the viscoelastic properties of PEEK/IM7 unidirectional laminae with different fiber orientation angles were investigated by sweeping the frequency across a range of 2 decades (0.1 Hz to 10 Hz) at room temperature (20C). The storage modulus and loss factor (tan δ) data, from the two specimens of PEEK/IM7 tested for different fiber orientation angles, and the corresponding curve fits are presented in Figures 12-14. It was found that as the frequency was increased there was a decrease in tan δ (damping) and a slight increase in the dynamic moduli (Storage or Loss Moduli). Damping, tan δ, is considerably more responsive to changes in frequency than storage modulus [25]. At low frequencies polymeric materials flow more, acting in a similar fashion to the flow at elevated temperatures, thus showing larger damping [13].

Figure.12: Frequency data for unidirectional beams with fibers oriented at 0' [13].

Figure.13: Frequency data for unidirectional beams with fibers oriented at 30' [13].

Figure.14: Frequency data for unidirectional beams with fibers oriented at 90' [13].

2.2. Viscoelastic Properties of Flexible Matrix Composite (FMC) Lamina

This section presents the technique used to determine the viscoelastic properties of a FMC lamina. After finding the complex shear and extensional moduli of the matrix material (polyurethane), the in-plane viscoelastic properties of FMC lamina can be evaluated using the Principle of Correspondence and the Micromechanics Approach [27].

2.2.1. Correspondence Principle

The correspondence principle states that the linear elastostatic analysis can be converted to dynamic linear viscoelastic analysis by replacing static stresses and strains with corresponding dynamic stresses and strains, and by replacing elastic moduli or compliances with complex moduli or compliances respectively [16]. This method has been employed to predict the damping in aligned discontinuous or continuous fiber-reinforced composites [17]. Correspondence principle has also been used in combination with the classical lamination theory [CLT] to determine the loss factor of laminated composites. The extensional (shear) loss factor has been expressed as a ratio of the imaginary extensional (shear) stiffness (E'' or G'') to the real extensional (shear) stiffness (E' or G') for a lamina [16].

$$\eta = \frac{E''}{E'}$$

(9)

2.2.2. Micro-Mechanics

Micromechanics is concerned with the study of composite materials on the level of the individual constituents that constitute these materials [18]. Micromechanics can be used to predict stiffness and strength (with lesser success) of a lamina. Micromechanical approach has been used for both continuous and short fiber reinforced composite materials.

Some basic concepts and definitions used in our research are described in the section:-

a) Volume and Mass Fractions – The properties of the composite are controlled by the relative volume of the fiber and matrix used. The fiber volume fraction is defined as

$$V_f = \frac{Volume\,of\,Fiber}{Total\,Volume}$$

(10)

The amount of matrix by volume is the matrix volume fraction, can be defined as

$$V_m = \frac{Volume\,of\,matrix}{Total\,Volume}$$

(11)

Since the total volume is the sum of the fiber volume plus the matrix volume, we have

$$V_f + V_m = 1$$

(12)

The amount of fiber by weight in the composite of the fiber weight fraction

$$W_f = \frac{Weight\,of\,fiber}{Total\,Weight}$$

(13)

The amount of matrix by weight (mass) is the matrix weight fraction

$$W_m = \frac{Weight\,of\,matrix}{Total\,Weight}$$

(14)

Similarly, since the total weight is the sum of the fiber weight plus the matrix weight,

$$W_f + W_m = 1$$

(15)

In the design of composite structures, volume fractions are used because they enter directly in the computations of stiffness. But during processing, weight fractions are used because it is much easier to weigh the components to be mixed than to measure their volume [14].

b) Longitudinal Modulus - The longitudinal modulus is the modulus of elasticity in the fiber direction and can be predicted using the Rule of Mixture (ROM) formula [26]. The main assumption in this formulation is that strains in the direction of fibers are the same in both the matrix and the fiber, i.e. the fiber-matrix bond is perfect [18].

$$E_1 = E_m V_m + E_f V_f$$

(16)

where E_1 is the longitudinal modulus (or modulus in the fiber direction), E_m is the modulus of the matrix material, E_f is the modulus of fiber material, V_f and V_m are the volume fractions of fibers and matrix materials, respectively.

c) Transverse Modulus (E_2) - The transverse modulus is the modulus of elasticity in a direction transverse to the fibers and can be predicted using the Inverse Rule of Mixtures (IROM)

formula. The main assumption in this formulation is that the stress in the direction transverse to the fibers is same in the fibers and matrix [18].

$$\frac{1}{E_2} = \frac{V_m}{E_m} + \frac{V_f}{E_f}$$ (17)

where E_2 is the transverse modulus.

d) In-Plane Poisson's Ratio (ν_{12}) - The Poisson's Ratio is defined as the negative ratio of the resulting strain vs the applied strain, i.e. in a test in which load is applied in the *i*-direction, strain induced by Poisson's effect on the perpendicular *j*-direction [18].

$$\nu_{ij} = -\frac{\epsilon_i}{\epsilon_j}$$ (18)

The Mechanics of Materials approach leads to the rule of mixture equation for the in-plane Poisson's Ratio

$$\nu_{12} = \nu_f V_f + \nu_m V_m$$ (19)

An approximate prediction of Poisson's ratio is usually sufficient in design, in general the Poisson's ratio for the matrix and the fibers are not very different [18].

e) In-Plane Shear Modulus (G_{12}) – A simple Strength of Material approach leads to the inverse rule of mixtures equation for the in-plane shear modulus [18].

$$\frac{1}{G_{12}} = \frac{V_m}{G_m} + \frac{V_f}{G_f}$$ (20)

The inverse rule of mixtures gives a simple but less accurate equation for the prediction of the in-plane shear modulus. The Tsai Hahn gives a better approximation [18],

$$G_{12} = G_m \left[\frac{1 + \zeta \eta V_f}{1 - \eta V_f} \right]$$ (21a)

$$\eta = \frac{(G_f/G_m) - 1}{(G_f/G_m) + \zeta}$$ (21b)

2.2.3. Ply-Mechanics

The main objective of ply mechanics is to present the constitutive equations of a lamina (also called ply) randomly oriented with respect to a reference co-ordinate system [16]. A review of the coordinate transformations and constitutive equations for a lamina are discussed below.

a) **Coordinate Systems**

There are two coordinate systems that are used in the composite design. The material coordinate system (denoted by axes 1, 2, 3), that has 1-axis aligned with the fiber direction, the 2-axis is the axis perpendicular to the fiber direction. Each lamina has its own material coordinate system aligned with the fiber direction. The global coordinate system (laminate coordinate system, denoted by x, y, z) is common to all the laminae in the laminate as shown in Figure 15. The orientation of the laminate system is chosen for convenience during structural analysis [18].

Figure.15: Coordinate relations between material axes (1, 2 and 3) and reference axes (x, y and z) [22].

b) Stress-Strain Equations

Most composite materials are used in the form of plates and shells, which have two major dimensions (length and width) much larger than the third dimension (thickness). When thickness of a composite plate is reasonably small as compared to the other dimensions, it is safe to assume that the transverse stress is zero (i.e. $\sigma_3 = 0$).

When a stress (σ_1) is applied along the fiber direction (1-axis) as shown in Figure 15, the strain can be computed as

$$\epsilon_1 = \frac{\sigma_1}{E_1}$$

(22)

And when applying a transverse stress (σ_2), the strain in the fiber direction is computed using the Poisson's Ratio,

$$\epsilon_1 = -\nu_{21}\epsilon_2 = -\nu_{21}\frac{\sigma_2}{E_2}$$

(23)

From the principle of superposition, the total resulting strain due to both stresses, in the fiber direction is,

$$\epsilon_1 = \frac{\sigma_1}{E_1} - \nu_{21}\frac{\sigma_2}{E_2}$$

(24)

Repeating the procedure along the transverse direction,

$$\epsilon_2 = \frac{\sigma_2}{E_2} - \nu_{12}\frac{\sigma_1}{E_1}$$

(25)

The shear terms are obtained directly from the shear version of the Hooke's Law,

$$\sigma_6 = \tau_{12} = G_{12}\gamma_6$$

(26)

$$\sigma_4 = \tau_{23} = G_{23}\gamma_4$$

(27)

$$\sigma_5 = \tau_{13} = G_{23}\gamma_5$$

(28)

Assuming that the composite material is transversely isotropic (i.e. they have the same properties in one plane (2-3 Plane) but different properties in a direction normal to this plane (1-plane)), we have the compliance equations as,

$$\begin{pmatrix} \epsilon_1 \\ \epsilon_2 \\ \gamma_{12} \end{pmatrix} = \begin{bmatrix} \frac{1}{E_1} & \frac{-\nu_{21}}{E_2} & 0 \\ \frac{-\nu_{12}}{E_1} & \frac{1}{E_2} & 0 \\ 0 & 0 & \frac{1}{G_{12}} \end{bmatrix} \begin{pmatrix} \sigma_1 \\ \sigma_2 \\ \tau_{12} \end{pmatrix}$$

(29)

and

$$\begin{pmatrix} \gamma_4 \\ \gamma_5 \end{pmatrix} = \begin{bmatrix} \frac{1}{G_{23}} & 0 \\ 0 & \frac{1}{G_{13}} \end{bmatrix} \cdot \begin{pmatrix} \sigma_4 \\ \sigma_5 \end{pmatrix} \tag{30}$$

Since the compliance must be symmetric [12], we have

$$\frac{\nu_{21}}{E_2} = \frac{\nu_{12}}{E_1} \tag{31}$$

The stresses σ_4 and σ_5 are neglected if the sample is very thin. The compliance equations (29) and (30) can be written in compact forms as,

$$\epsilon = [S].\sigma \tag{32}$$
$$\gamma = [S^*].\tau \tag{33}$$

Where, [S] is called the compliance Matrix and [S*] is the inter-laminar compliance matrix.

$$[S] = \begin{bmatrix} \frac{1}{E_1} & \frac{-\nu_{12}}{E_1} & 0 \\ \frac{-\nu_{12}}{E_1} & \frac{1}{E_2} & 0 \\ 0 & 0 & \frac{1}{G_{12}} \end{bmatrix} \tag{34}$$

$$[S^*] = \begin{bmatrix} \frac{1}{G_{23}} & 0 \\ 0 & \frac{1}{G_{13}} \end{bmatrix} \tag{35}$$

c) Coordinate Transformation

Most composite structures have more than one lamina because the properties in the transverse direction of a lamina are relatively low when compared to the longitudinal properties. Therefore, several laminae are stacked in different orientations so that reinforcements (fibers) are placed along all directions of loading. For a specific kind of loading (axial, shear), the stress vector in the global coordinate system (Laminate Coordinate system) is given or can be determined. Using the transformation matrix [T], the strain vector in the material coordinate system can be computed for any fiber angle orientation (Θ_f), as follows,

$$\begin{pmatrix} \epsilon_1 \\ \epsilon_2 \\ \gamma_{12} \end{pmatrix} = [T]. \begin{pmatrix} \epsilon_x \\ \epsilon_y \\ \gamma_{xy} \end{pmatrix} \tag{36}$$

where [T] is the transformation matrix and m=Cos (θ) and n=Sin (θ)

$$[T] = \begin{bmatrix} m^2 & n^2 & mn \\ n^2 & m^2 & -mn \\ -2mn & 2mn & m^2 - n^2 \end{bmatrix} \tag{37}$$

2.3. Viscoelastic Properties and Effective Damping of a FMC Laminate.

Most composite structures are built with laminates having several laminae with various orientations as shown in Figure. 3. The lamina orientations are chosen to provide adequate stiffness and strength in the direction of the applied loads, taking into account that the composite material is much stronger and stiffer in the fiber direction than in any other direction.

2.3.1. Viscoelastic Properties of a FMC Laminate

The correspondence principal in accordance with the Classical Lamination Theory (CLT) is used to determine the viscoelastic properties of a Polymer Matrix Composite (PMC) laminate. The thickness of a laminate is small compared to the in-plane dimensions (i.e. length and width) of the plate, every lamina is in a state of stress. Therefore, the stress strain relations in the material coordinate system is given by,

$$
\begin{pmatrix} \epsilon_1 \\ \epsilon_2 \\ \gamma_{12} \end{pmatrix}^k = \begin{bmatrix} S_{11} & S_{12} & 0 \\ S_{12} & S_{22} & 0 \\ 0 & 0 & S_{66} \end{bmatrix}^k \begin{pmatrix} \sigma_1 \\ \sigma_2 \\ \tau_{12} \end{pmatrix}^k
$$

(38)

Or

$$
\begin{pmatrix} \sigma_1 \\ \sigma_2 \\ \tau_{12} \end{pmatrix}^k = \begin{bmatrix} Q_{11} & Q_{12} & 0 \\ Q_{12} & Q_{22} & 0 \\ 0 & 0 & Q_{66} \end{bmatrix}^k \begin{pmatrix} \epsilon_1 \\ \epsilon_2 \\ \gamma_{12} \end{pmatrix}^k
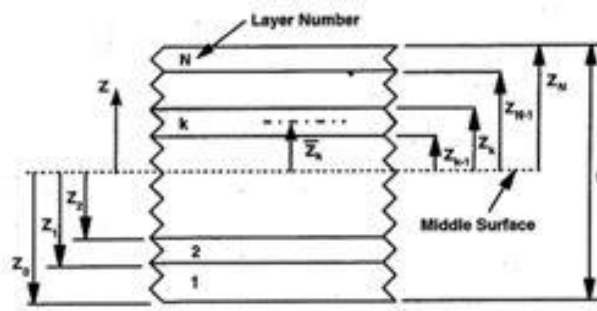$$

(39)

Figure.16: Geometry of a laminate with N laminae [18].

where the superscript k indicates the lamina number as shown in Figure 16 and [Q] is the stiffness matrix, [Q] =inverse [S]. The stress-strain relation in laminate coordinates is given by,

$$\begin{pmatrix} \sigma_x \\ \sigma_y \\ \sigma_{xy} \end{pmatrix}^k = \begin{bmatrix} \overline{Q}_{11} & \overline{Q}_{12} & \overline{Q}_{16} \\ \overline{Q}_{21} & \overline{Q}_{22} & \overline{Q}_{26} \\ \overline{Q}_{16} & \overline{Q}_{26} & \overline{Q}_{66} \end{bmatrix}^k \begin{pmatrix} \epsilon_x \\ \epsilon_y \\ \epsilon_{xy} \end{pmatrix}^k$$

(40)

where, $\overline{Q}$ is the reduced transformed stiffness matrix and is given by,

$$[\overline{Q}] = [T]^{-1}[Q][R][T][R]^{-1}$$

(41)

And,

$$[R] = \begin{bmatrix} 1 & 0 & 0 \\ 0 & 1 & 0 \\ 0 & 0 & 2 \end{bmatrix}$$

(42)

In case of a laminate made up of several layers of homogenous anisotropic materials the constitutive equation can be written as,

$$\begin{pmatrix} N \\ M \end{pmatrix} = \begin{bmatrix} A & B \\ B & D \end{bmatrix} \begin{pmatrix} \epsilon^0 \\ k \end{pmatrix}$$

(43)

where,

$$[N] = \begin{bmatrix} N_x \\ N_y \\ N_{xy} \end{bmatrix} [M] = \begin{bmatrix} M_x \\ M_y \\ M_{xy} \end{bmatrix} [\epsilon^0] = \begin{bmatrix} \epsilon_x^0 \\ \epsilon_y^0 \\ \gamma_{xy}^0 \end{bmatrix} [k] = \begin{bmatrix} k_x \\ k_y \\ k_{xy} \end{bmatrix}$$

(44)

[N] and [M] are the force and moment vectors resultants acting on a section (per unit length), [ϵ^0] and [k] are the in-plane strain and curvature vectors.

In equation 42, [A] is the in-plane stiffness matrix because it directly relates the in-plane strains to the in-plane forces,

$$[A] = \begin{bmatrix} A_{11} & A_{12} & A_{16} \\ A_{12} & A_{22} & A_{26} \\ A_{16} & A_{26} & A_{66} \end{bmatrix}, A_{ij} = \sum_{k=1}^{N}(\overline{Q}_{ij})_k(z_k - z_{k-1}); i,j = 1,2,6$$

(45)

[B] is the bending extension coupling matrix since it relates the in-plane strains to bending moments and curvatures to the in-plane forces

$$[B] = \begin{bmatrix} B_{11} & B_{12} & B_{16} \\ B_{12} & B_{22} & B_{26} \\ B_{16} & B_{26} & B_{66} \end{bmatrix}, B_{ij} = \frac{1}{2}\sum_{k=1}^{N}(\overline{Q}_{ij})_k(z_k^2 - z_{k-1}^2); i,j = 1,2,6$$
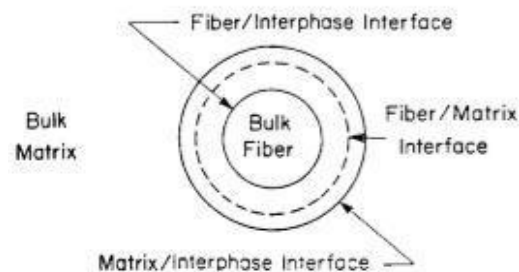
(46)

and [D] is the bending stiffness matrix because it directly relates the curvatures to bending moments.

$$[D] = \begin{bmatrix} D_{11} & D_{12} & D_{16} \\ D_{12} & D_{22} & D_{26} \\ D_{16} & D_{26} & D_{66} \end{bmatrix}, D_{ij} = \frac{1}{3}\sum_{k=1}^{N}(\overline{Q}_{ij})_k(z_k^3 - z_{k-1}^3); i,j = 1,2,6$$

(47)

2.3.2. Effective Damping in a FMC Laminate

Damping is an important parameter related to the study of dynamic behavior in fiber-reinforced composite structures [16]. It can be defined as the dissipation of energy in a material under cyclic load [9]. Damping mechanisms in composite materials are completely different from those in conventional metals and alloys [16]. In the automobile and aerospace industry considerable amount of research is being done to improve the damping of mechanical vibrations which can be achieved in three ways, (i) removing or isolating the source of vibration, (ii) Changing the mass and/or stiffness of the structure which intern will increase or decrease the natural frequency of the structure, and (iii) Absorbing the vibrational energy [20]. Some of the different sources of energy dissipation are: -

1. Viscoelastic Nature of Matrix and/or Fiber Materials - Most of the damping in composite materials is attributed to the matrix, however the damping due to fibers must also be taken into account while dealing with carbon and kevlar fibers since these fibers possess the highest damping when compared to other fiber materials [16].

2. Damping due to Interphase - Interphase is the region adjacent to the fiber surface along the entire length of the fiber [19] as shown in Figure 17. The nature of the interphase accordingly affects the mechanical properties as well as the damping characteristics of the fiber reinforced composites [16].

Figure.17: An ideal representation of Interface [19].

3. Damping due to Damage - There are two types of damping due to damage, (i) frictional damping mainly due to slip in the unbound regions between the fibers and matrix interface and (ii) damping due to energy dissipation in the area of matrix cracks or broken fibers [16].

4. Visco-plastic Damping – At large amplitudes of vibration and high stress levels, especially for thermoplastic materials, materials exhibit an evident degree of non-linear damping due to the presence of high stress and strain concentration that exist in local regions between fibers[16].

5. Thermo-elastic Damping - Occurs due to the cyclic heat flow from a region of compressive stress to the region of tensile stress in the composite. Thermoplastic composites show

high temperature rise which is a function of applied load, frequency, sample thickness and number of cycles [16].

In this research we consider damping due to the viscoelastic nature of the matrix and, we neglect the damping effects of the fiber (carbon) since when compared to the damping in the matrix, especially polyurethane (PU), the damping due to fibers is negligible [16].

2.3.3. Analytical Prediction of Damping

Many analytical models for the prediction of damping at micromechanical, macro-mechanical and structural level are based on the assumption of linear viscoelasticity. Adams and Bacon [21] developed a macro-mechanical model for damping in unidirectional fiber-reinforced composites which is being referred to as Adams-Bacon criteria. It states that the sum total of energy dissipated in a unidirectional lamina is equal to the energy dissipated separately by longitudinal stress, transverse stress and shear stress [16].

A widely recognized method for predicting the composite damping behavior in a laminate is the Strain Energy Method, which can be viewed as a special case of Adams-Bacon criteria. This method relates the total damping in the material or structure to the damping of each element and the fraction of the total strain energy stored in that element [16]. According to this theory for any system of linear viscoelastic elements the loss factor can be expressed as a ratio of summation of the product of individual element loss factor and strain energy stored in each element to the total strain energy [16]. When applying these methods to composites, the composite becomes a system, and on the nature of element depends whether the analysis is micro-mechanical or macro-mechanical [16]. In micromechanical analysis the elements include the constituents such as fibers, matrix and their interaction, void content and the interphase. On the other hand for macro-mechanical analysis, the individual lamina are the elements whose strain and dissipation energies combine to give the overall loss factor of the laminate [16]. In our research the effective extensional and shear loss factors of the laminate are considered. Using the classical lamination theory, complex A-B-D matrices are obtained and longitudinal, transverse and shear loss factors are determined. Accordingly, the effective loss factor (η) is given by,

$$\eta = \frac{W^d}{W^e} = \frac{\sum_k W_k^d}{\sum_k W_k^e} \tag{48}$$

where W^e is the total elastic strain energy (energy stored) per cycle of loading, W^d is the total dissipated energy per cycle and k is the lamina (ply) number and the specific damping capacity is an alternate measure of damping for laminates.

If W is the total work done per cycle, then

$$W = \sum_k W_k = \sum_k (W_k^e + iW_k^d) = \sum_k \frac{1}{2} \int \sigma_k \epsilon_k dV$$

<div align="right">(49)</div>

where σk and εk are the in-plane stress and strain vectors in the material co-ordinates for lamina k.

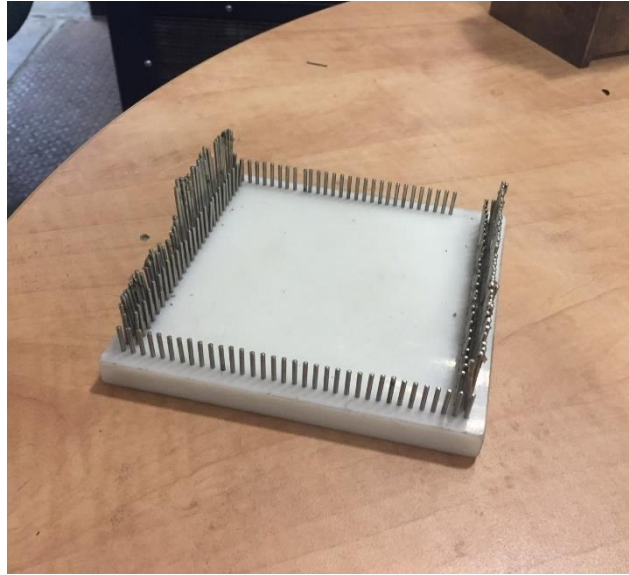# Chapter 3

Experimental Work and Discussions

The primary objective of the experimental work is to manufacture a 3-layer Carbon-Polyurethane laminate and find its viscoelastic characteristics. Section 3.1, introduces the manufacturing process used to make the 3-layer laminate. Secondly, Section 3.2 introduces the DMA test procedure. Section 3.3 discusses the extensional and shear moduli of the matrix Polyurethane (PU). Section 3.4 discusses the viscoelastic properties of a Carbon-Polyurethane (PU) lamina and finally section 3.5 discusses the viscoelastic properties of a sample 3-Layer laminate.

3.1. The Manufacturing Procedure.

The manufacturing of the laminate is a combination of both the filament winding and hand lay-up process. It may be viewed as a manual layup (fiber placing) process. In this work, the Hexcel M40JB 12K carbon fibers and the Smooth-On PMC® 121-30 urethane rubber (matrix) are used. It is also important to note that urethane rubber is made by the mixture of pre-polymer (Part-A) and curative (Part-B) at an 1:1 ratio by volume, and takes roughly 30 minutes to solidify and about 16 hours to fully cure (Curing is a chemical process of hardening of a polymer material).

Following are the main steps for the manufacturing of the FMC laminate: -

1. A flat plate is used as a base (open mold) for the manual placing of the fiber. Dowell pins are placed at specific intervals as shown in Figure 18 and details of the drawing are displayed in the Appendix B. These pins guide the manual fiber placing process at the proper orientation angles. Guided by the pins the fibers are manually placed at the required orientation angle as shown in Figure 19. During the layup process the fibers are witted with the PU resin using a brush so that it is evenly distributed and every fiber is properly saturated with resin. A fiber and matrix volume fraction between 0.3 to 0.35 and 0.7 to 0.65, respectively, are used. It is difficult to maintain the same volume fraction since different batches of samples were employed. For the analysis a constant fiber volume fraction of 0.33 was used.

Figure.18: Teflon plate with dowel (guide) pins.

2. The process is repeated for the second layer. In order to ensure a proper adhesion between the two layers, the second layer is placed on top of the first layer before the process of curing (Curing is a chemical process of hardening of a polymer material) is completed.

Figure.19: The laminate under manufacturing.

3. Once the three layers are placed (Figure 20), the laminate together with the plate are pressed (by a hydraulic press) under an optimum pressure of two metric tons in order to consolidate the layers and achieve good inter-laminar bonding. Care is taken to apply only the required pressure in order to avoid disorienting the fibers. The laminate along with the mold are left in the hydraulic press for a few days to cure.
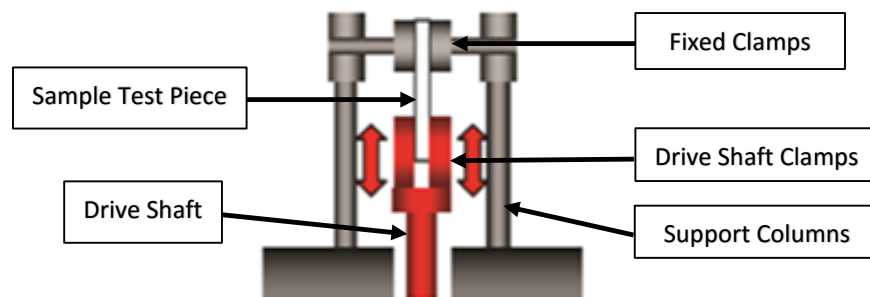
Figure.20: Completed laminate structure.

4. Once the curing press is complete, the mold is taken out of the press. The guide pins are carefully removed and the laminate is ready for use.
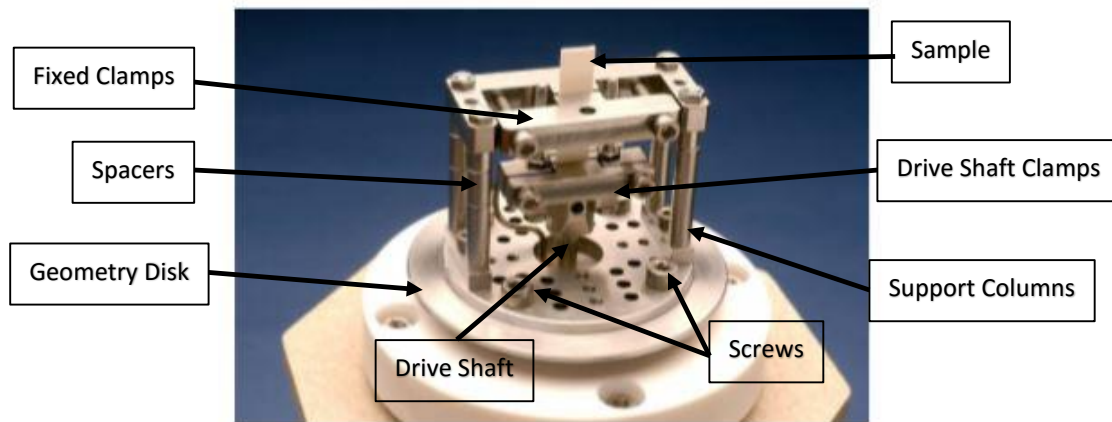
3.2. DMA Test Procedure.

This section briefly discusses the various steps involved in setting up the DMA-8000 to perform the tension and the shear test in general. In tension the geometry of the sample is being pulled. It is most useful for thin films and fiber analysis. The sample is anchored on one end by a fixed clamp and by the drive shaft on the other. Tension stress is being applied by the drive shaft (mounted on the motor) as shown in Figure 21. The DMA control software is used to apply a force of 1N. The fixtures required to perform the tension test on the sample were readily available.

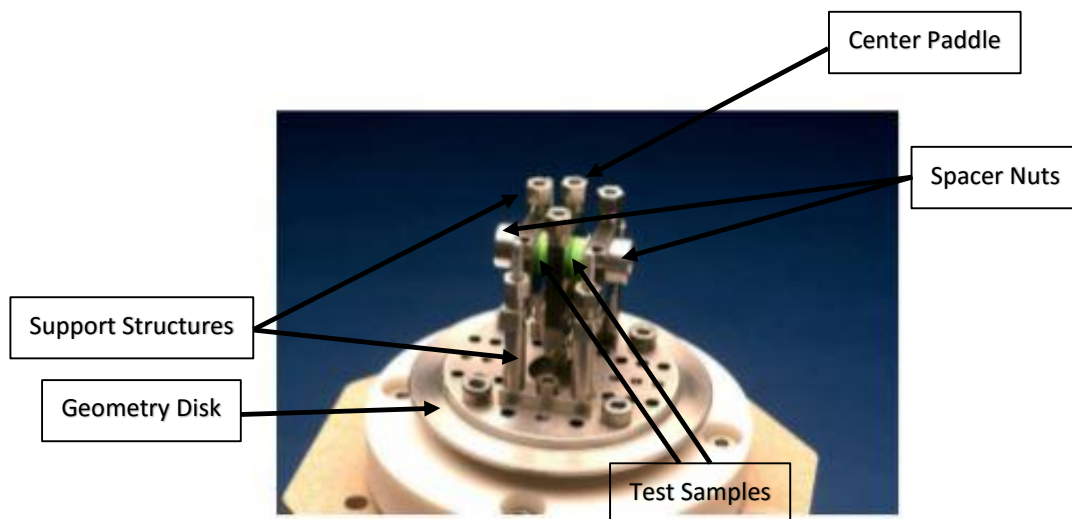**Figure.21:** Schematic depicting the tension test fixtures.

Figure 22 shows the actual tension test fixtures. The tension geometry may require loosening and rotation of the geometry disk to get the required set of holes vertically aligned. This is done by loosening the four screws holding the geometry disk to the insulating disk and gently rotating

it to the appropriate position. The support structures are placed as shown. The sample length is determined by the spacers provided in the kit.

Figure.22: The tension test fixtures.

Figure 23 shows the actual set up of the shear fixture. In the shear test two identical samples are gently squeezed between two side plates and a center paddle which is screwed to the drive shaft (Figure 24).It should be mentioned that the shear fixture is a little counter intuitive to setup. The setup of the gap between the side plates and the center paddle depends on the nature of the sample (solids, rubber like foams or liquids). An optimum pressure needs to be applied which is sufficient enough to prevent slipping of the sample, without affecting the applied shearing.

Figure.23: Final arrangement of the shear test fixtures.

Figure.24: Schematic depicting the shear test fixtures.

Figure 25 shows the actual set up of the 3pt-bending fixture. In the 3-pt bending test the samples are placed on the outer knife edges without being clamped. A center knife driven by the drive shaft is placed on the sample right at the center (Figure 26). The nuts on the center knife should be adjusted such that it remains in contact across the entire width of the sample. It is used for accurate modulus values for very stiff, high modulus materials, i.e., steel, and composites.

Figure.25: Final arrangement of the 3-pt bending test fixtures.

Figure.26: Schematic depicting the 3-pt bending test fixtures.

It should also be mentioned that the fixtures required to perform the shear test on the sample were missing. The fixtures were designed, drawn using SolidWorks, and manufactured in our machine shop. The fixtures were made out of stainless steel and were manufactured using precision manufacturing techniques. The schematic of the fixture is shown in Figure 27, and details of the drawing are displayed in the Appendix B.

Figure.27: Shear test fixtures created using Solidworks.

The choice of the geometry to run the sample in is dictated by the sample's physical state at the beginning of the experiment. Table 1 shows the geometry of the sample selected for the tension, shear and bending test.

	Tension Test	Shear Test	Bending Test
Geometry of Sample	Rectangular	Circular	Rectangular
Length [Diameter] (mm)	10.9	10	20
Width (mm)	7.4	Nil	10
Thickness mm)	2.33	2.06	2
Frequency Range (Hz)	1-100	1-100	1-100
Points/Decade	5	5	5
Temperature Range (K)	263-313	263-313	263-313

Table.1: Sample geometry for different tests.

3.3. Extensional and Shear Moduli of Polyurethane (PU).

Samples of the results of the work done for polyurethane (PU) are presented below [28]. The DMA measures the variation of the storage and loss moduli of a viscoelastic material as a function of frequency over a range of temperature. The Time-Temperature Superposition (TTS) principle is applied to generate the master curve [23] that represents the extensional (shear) modulus vs the 'Reduced Frequency', $f\alpha_t$. The TTS principle uses the William-Landel-Ferry (WLF) Shift factor, α_t [9] to collapse the moduli curve at various temperatures onto the master curve.

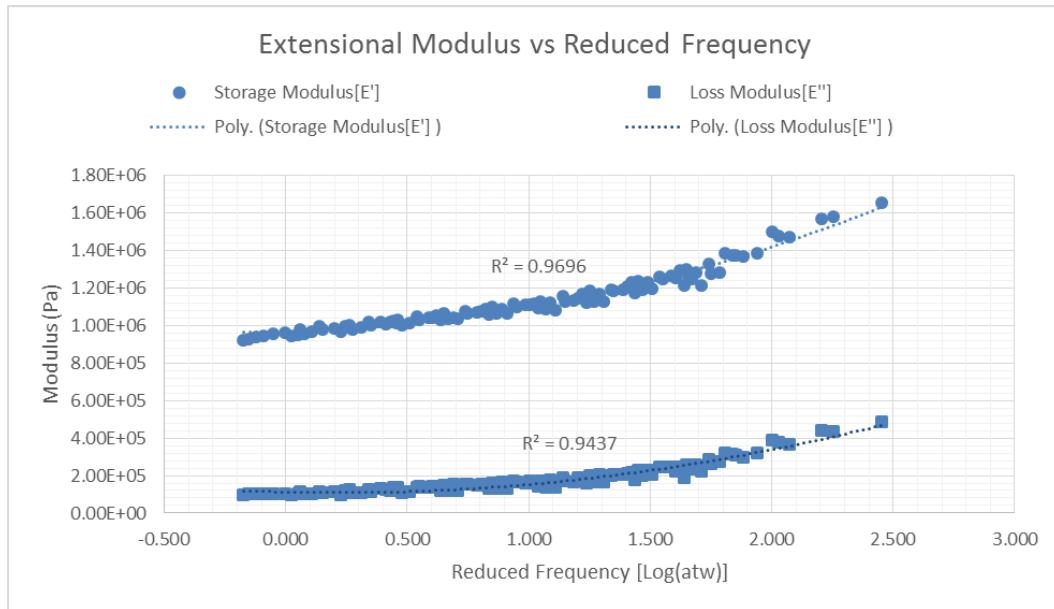$$log(\alpha_t) = -\frac{C_1(T - T_0)}{C_2 + T - T_0}$$

(52)

where C_1 and C_2 are material constants to be determined experimentally, T is temperature in Kelvin and T_0 is the reference temperature on which the master curves are created.

The complex shear (G^*) and extensional (E^*) moduli are given by,

$$E^*(x) = E'(x) + iE''(x)$$

(53)

$$G^*(x) = G'(x) + iG''(x)$$

(54)

where, E' is the extensional storage modulus, E'' is the extensional loss modulus, G' is the shear storage modulus and G'' is shear loss modulus. The results of the extensional and shear moduli along with the loss tangent [Tan(δ)] (for both extensional and shear modulus) are presented in Figures 28, 29, 30 and 31, respectively. A sample of the plot of the raw data is shown in Appendix C. It is important to note that no peaks are experienced for the loss modulus and loss factor. This is because the glass transition temperature, where the peak normally occurs is significantly below the range of temperatures studied in this work.

Figure.28: The dynamic extensional storage and loss modulus.

Figure.29: The dynamic shear storage and loss modulus.

Figure.30: The loss tangent [Tan(δ)] for extensional moduli.

Figure.31: The loss tangent [Tan(δ)] for shear moduli.

Since polyurethane (PU) is a homogenous material, the Poisson's Ratio can be calculated using,

$$\nu^*(x) = \frac{E^*(x)}{2 * G^*(x)} - 1$$

(54a)

The plot of Poisson's Ratio vs Frequency is shown in Figure 32. Notice that the imaginary Poisson's Ratio (ν'') is negligible compared to the real part and consequently may be treated as real; an observation confirmed by Victor et al [29]. Also note that the Poisson's Ratio is more than 0.5. For a rubbery viscoelastic material like polyurethane the Poisson's Ratio is approximately 0.5 [29], which suggests that the measurement of the modulus (E* or G*) may not be accurate.

Figure.32: The Poisson's Ratio for Polyurethane(PU).

It should be mentioned that determination of the Poisson's ratio as a function of time and/or frequency is extremely difficult. Because of the considerable experimental difficulties, information on this function is still rather scanty. In addition, even this scant literature is replete with reports of work based on incorrect equations. In general, the determination of any bulk functions by calculation from any other parameters requires the source parameters to be obtained using a strict protocol known as the standard protocol [30]. The standard protocol states that the source parameters be determined simultaneously on the same specimen, under the same conditions of the experimental environment. This guarantees identical initial and final boundary conditions along with high accuracy and precision [30].

Thus, viscoelastic Poisson's ratio cannot be calculated indirectly by combining response functions such as E*(ω) and G*(ω), obtained from separate measurements. If any bulk response function is to be calculated from two other response functions, it is absolutely mandatory that the source functions be determined in accordance with the Standard Protocol. This demands that highly accurate measurements be made on the same specimen, at the same time, and under the same conditions of the experimental environment. This may require the construction of novel apparatus. It should be pointed out that the effect of Poisson's Ratio is negligible on the results presented. The four moduli and Tan(δ) values are approximated by a quadratic polynomial fit, that is
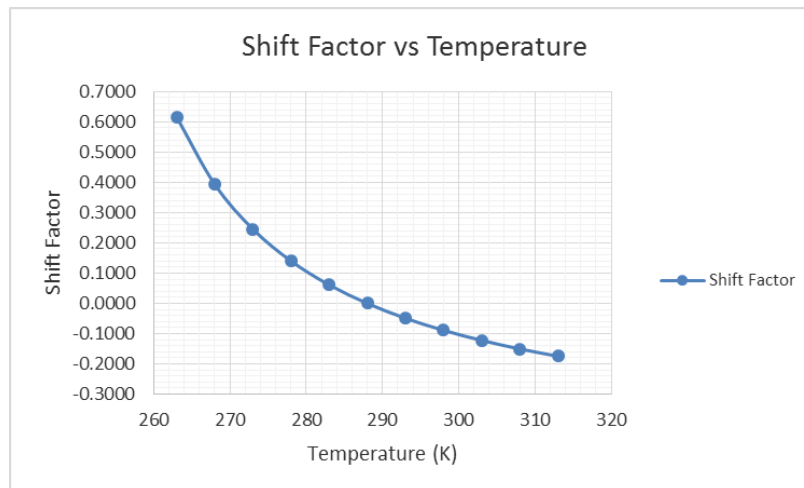
$$E = a_2 x^2 + a_1 x + a_0 \qquad (55)$$

where E stands for any of the four moduli or damping depending on the type of loading, α_t is the WLF Shift Factor and x is the frequency. The values of the material constants a_2, a_1, a_0, C_1 and C_2 are shown in Table 2.

	a_2	a_1	a_0	Standard Deviation	WLF Constants	
E' (KPa)	97.61	31.12	965.2	6.65E+04	C_1	0.47
E''(KPa)	71.51	-30.41	111.84	4.47E+04	$C_2(^0K)$	43.36
η [Tan(δ)]	0.03	-6E-05	0.11	3.51E-02		
G'(KPa)	15.49	24.08	259.32	2.38E+04	C_1	0.53
G''(KPa)	13.26	-0.84	26.03	5.92E+03	$C_2(^0K)$	46.45
η [Tan(δ)]	0.027	0.002	0.01	1.28E-02		

Table.2: Material properties of the extensional and shear moduli.

The corresponding shift factor versus temperature for tension and shear test respectively, are shown in Figure 33.

(a)

(b)

Figure.33: A plot of shift factor vs temperature (a) Tension test (b) Shear test.

3.4. Viscoelastic Properties of a Carbon-Polyurethane Lamina.

After finding the complex extensional (E^*) and shear (G^*) moduli of the matrix material (polyurethane), the next step is to determine the in-plane viscoelastic characteristics of a Carbon-Poly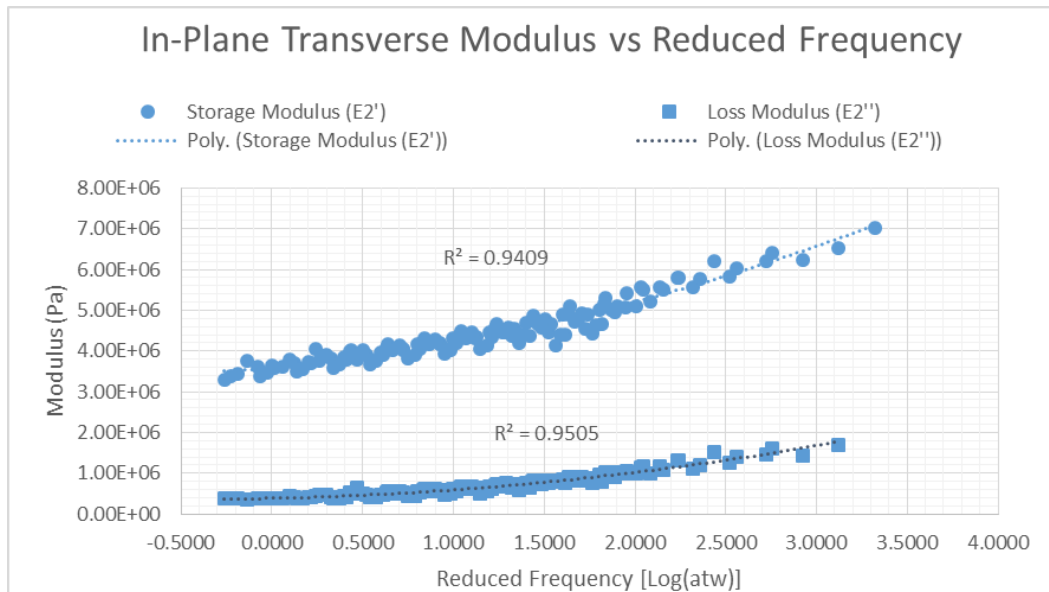urethane (PU) lamina experimentally, and to compare it with the analytical models used. In these experiments only properties such as effective transverse complex modulus (E_2^*) and the effective in-plane shear modulus (G_{12}^*) were evaluated. The effective complex longitudinal modulus (E_1^*) was ignored because the complex longitudinal modulus (E_1^*) i.e. the elastic modulus in the direction of the fibers, is a fiber dominated property and is almost equal to the modulus of the fibers. The Dynamic Mechanical Analyzer (DMA 8000) used does not support the measurement of the effective in-plane Poisson's Ratio (v_{12}^*). It needs to be determined using other experiments, which is beyond the scope of this work. The complex in-plane transverse (E_2^*) and shear (G_{12}^*) moduli are given by,

$$E_2^*(x) = E_2'(x) + iE_2''(x)$$

(56)

$$G_{12}^*(x) = G_{12}'(x) + iG_{12}''(x)$$

(57)

where, E_2' is the in-plane transverse storage modulus, E_2'' is the in-plane transverse loss modulus, G_{12}' is the in-plane shear storage modulus and G_{12}'' is in-plane shear loss modulus. The results of the transverse elastic modulus and in-plane shear modulus are presented in Figures 34 and 35, respectively. The loss tangent (Tan(δ)) for the lamina for each of the types of loading are presented in Figures 36 and 37, respectively. A sample of the plot of the raw data is shown in Appendix C.

Figure.34: The dynamic in-plane transverse storage and loss modulus.

Figure.35: The dynamic in-plane shear storage and loss modulus.

Figure.36: The loss tangent [Tan(δ)] for transverse moduli

Figure.37: The loss tangent [Tan(δ)] for in-plane shear moduli.

The four moduli and the loss tangent are approximated by a quadratic polynomial fit, that is

$$E = a_2 x^2 + a_1 x + a_0$$

(58)

where E stands for any of the four moduli or the loss tangent value depending on the type of loading, α_t is the WLF Shift Factor and x is the frequency. The values of the material constants a_2, a_1, a_0, C_1 and C_2 are shown in Table 3.

	a_2	a_1	a_0	Standard Deviation	WLF Constants	
E' (KPa)	186.31	432.93	400	1.53E+05	C_1	0.67
E''(KPa)	115.09	87.53	388.61	5.56E+04	$C_2(^0K)$	37.61
η [Tan(δ)]	0.008	0.027	0.106	8.13E-03		
G'(KPa)	49.91	57.15	700.85	1.07E+04	C_1	0.34
G''(KPa)	41.26	-24.21	123.93	9.41E+03	$C_2(^0K)$	38.16
η [Tan(δ)]	0.026	0.021	0.172	9.61E-03		

Table.3: Material Properties of a carbon/polyurethane lamina.

The corresponding shift factor versus temperature for tension and shear test respectively, are shown in Figure 38.

(a)

(b)

Figure.38: A plot of shift factor vs temperature (a) Tension test (b) Shear test.

3.5. Viscoelastic Properties of a 3-Layer Carbon-Polyurethane (PU) Laminate.

After finding the complex transverse ($E_2{}^*$) and in-plane shear ($G_{12}{}^*$) moduli of a carbon-polyurethane lamina, the next step is to determine the material properties of a 3-layer laminate with fiber orientation angles equal to [θ/β/θ] and compare it with the analytical models used. According to Ghoneim and Zhen [2] in the manufacturing of a FMC pump, a high negative effective Poisson's ratio lies in the zone between θ= 0^0 to 5^0 and β= 10^0 to 50^0. A sample laminate of [θ/β/θ] equal to [5/35/5] was chosen. The DMA was used to measure the laminate modulus, i.e., extensional modulus in the X-direction (E_x), extensional modulus in the Y-direction (E_y), the in-plane shear modulus (G_{xy}) and the extensional bending modulus (E_b). But based on the preliminary analysis (as discussed in Section 4.2) it was found that the extensional modulus (E_x) in the X-direction and the shear modulus (G_{xy}) for a [5/35/5] laminate lies beyond the measurable range of the DMA. To accommodate this, another laminate with [θ/β/θ] equal to [30/-60/30], whose modulus lies within the measurable range of the DMA was selected. The laminates selected was manufactured using the steps discussed in section 3.1. Table 4 shows the type of laminate selected for measuring each of the laminate modulus.

Sl No.	Type of Modulus Measured	Type of Laminate Selected
1	Extensional Modulus in X-direction (E_x)	[30/-60/30]
2	Extensional Modulus in Y-direction (E_y)	[5/35/5]
3	In-Plane Shear Modulus (G_{xy})	[30/-60/30]
4	Extensional Bending Modulus (E_b)	[5/35/5]

Table.4: Types of laminates selected for experimentation.

The complex extensional ($E_x{}^*$), ($E_y{}^*$), shear ($G_{xy}{}^*$) and bending ($E_b{}^*$) moduli are given by
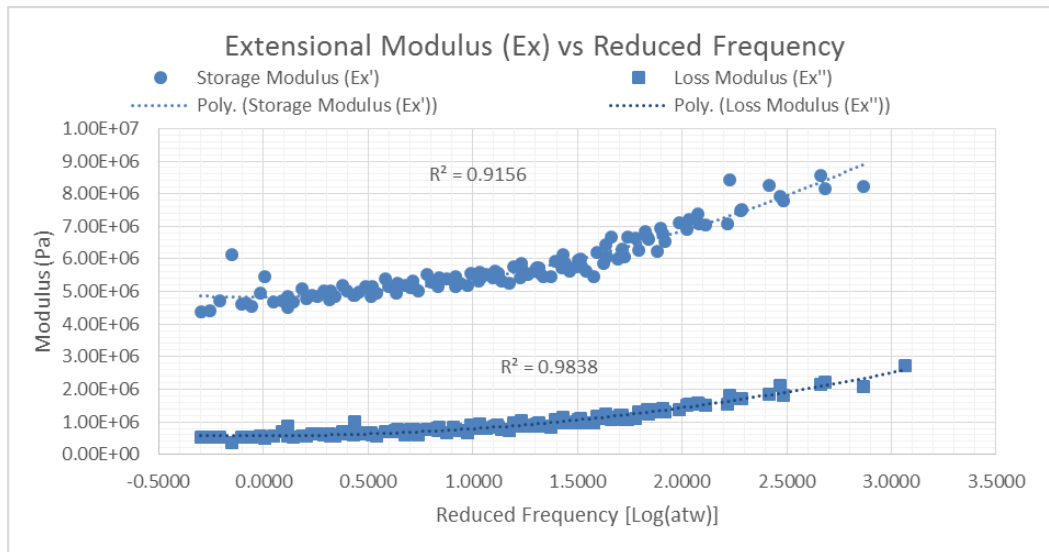
$$E_x^*(x) = E_x'(x) + iE_x''(x) \tag{59}$$

$$E_y^*(x) = E_y'(x) + iE_y''(x) \tag{60}$$

$$G_{xy}^*(x) = G_{xy}'(x) + iG_{xy}''(x) \tag{61}$$

$$E_b^*(x) = E_b'(x) + iE_b''(x) \tag{62}$$

where, E_x' is the in-plane longitudinal storage modulus, E_x'' is the in-plane longitudinal loss modulus (in the x-direction), E_y' is the in-plane transverse storage modulus, E_y'' is the in-plane transverse loss modulus (in the y-direction), G_{xy}' is the in-plane shear storage modulus, G_{xy}'' is in-plane shear loss modulus, E_b' is the bending storage modulus and E_b'' is the bending loss modulus. The results of the extensional modulus (both in X and Y direction), in-plane shear modulus and bending modulus are presented in Figures 39, 40, 41 and 42, respectively. The loss tangent (Tan(δ)) for the laminate for each of the types of loading are presented in Figures 43, 44, 45 and 46, respectively. A sample of the plot of the raw data is shown in Appendix C.

Figure.39: The laminate elastic (E_x) storage and loss modulus.

Figure.40: The laminate elastic (E_y) storage and loss modulus.

Figure.41: The laminate shear (G_{xy}) storage and loss modulus.

Figure.42: The laminate bending (E_b) storage and loss modulus.

Figure.43: The loss tangent [Tan(δ)] for laminate elastic moduli (E_x).

Figure.44: The loss tangent [Tan(δ)] for laminate elastic moduli (E_y).

Figure.45: The loss tangent [Tan(δ)] for laminate shear moduli (G_{xy}).

Figure.46: The loss tangent [Tan(δ)] for laminate bending moduli (E_b).

The six moduli and the loss tangent are approximated by a quadratic polynomial fit, that is

$$E = a_2 x^2 + a_1 x + a_0 \qquad (63)$$

where E stands for any of the four moduli or the loss tangent value depending on the type of loading, α_t is the WLF Shift Factor and x is the frequency. The values of the material constants a_2, a_1, a_0, C_1 and C_2 are shown in Table 5.

	a_2	a_1	a_0	Standard Deviation	WLF Constants	
E_x' (KPa)	385.23	306.99	500	2.65E+05	C_1	0.875
E_x''(KPa)	220.1	-8.11	579.69	9.91E+04	$C_2(^0K)$	44.5
η [Tan(δ)]	0.015	0.01	0.1198	0.011		
E_y' (KPa)	289.99	590.747	500	1.13E+05	C_1	0.86
E_y''(KPa)	214.929	0.404	577.3	5.44E+04	$C_2(^0K)$	44.5
η [Tan(δ)]	0.014	0.013	0.1189	0.01		
G_{xy}'(KPa)	188.70	433.40	400	1.24E+05	C_1	1.12
G_{xy}''(KPa)	124.45	66.12	398.74	4.19E+04	$C_2(^0K)$	41.85
η [Tan(δ)]	0.0135	0.0165	0.1097	0.00673		
E_b' (MPa)	30.00	20.00	2000.00	1.07E+04	C_1	1
E_b'' (MPa)	20.00	40.00	200.00	9.40E+03	$C_2(^0K)$	41.58
η [Tan(δ)]	0.0051	0.0184	0.1087	0.0096		

Table.5: The Laminate Material Properties.

The corresponding shift factor versus temperature for tension, shear and bending test, respectively, are shown in Figure 47.

(a)

(b)

(c)

(d)

Figure.47: A plot of shift factor vs temperature (a) Tension test (b) Tension test (c) Shear test (d) Bending test.

Chapter 4

Analytical Work and Discussions

The primary purposes of the analytical work are as follows: first, to find the in-plane viscoelastic properties of a Carbon/Polyurethane (C/PU) lamina and a laminate. Second, estimate the optimal fiber orientations and material properties for achieving a high effective damping. In this chapter, section 4.1 presents the analysis of the viscoelastic material properties of a Carbon-Polyurethane (PU) lamina; section 4.2 discusses the material properties of the laminated structure and section 4.3 studies the effective damping on a sample 3-layer laminate.
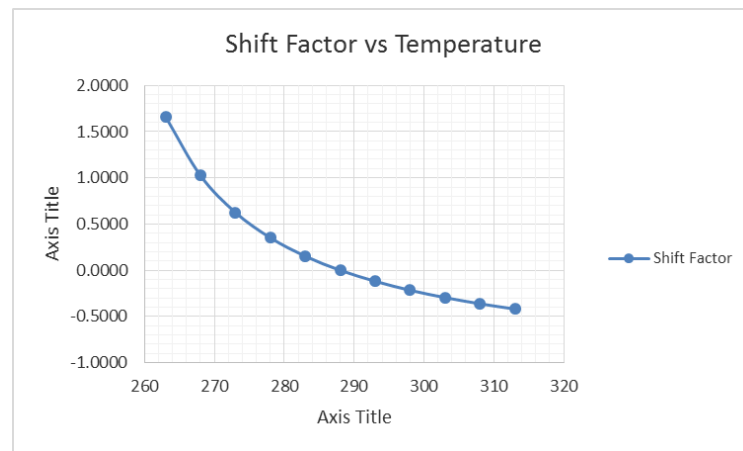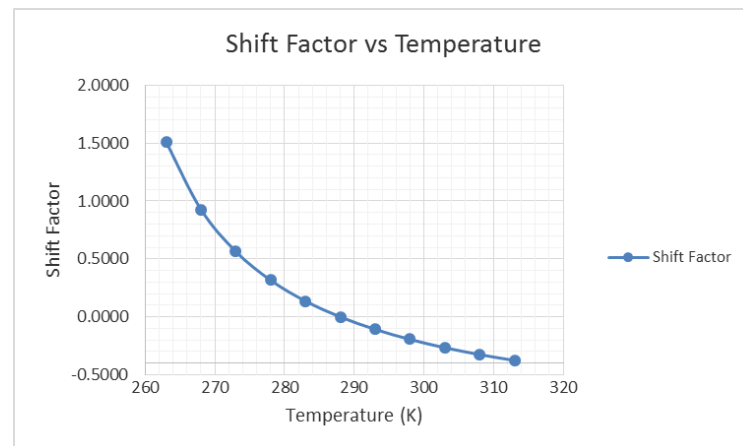
4.1. Viscoelastic Properties of a Carbon-Polyurethane (C/PU) Lamina using different Analytical Models.

After finding the complex extensional (E*) and shear (G*) moduli of the matrix material (polyurethane), the in-plane viscoelastic properties of the Carbon/Polyurethane lamina are evaluated using the Principle of Correspondence and the Micro-Mechanics Approach. We made certain assumptions while evaluating the in-plane characteristics:

1. Carbon fibers are considered to be purely elastic with an Elastic Modulus (E_f) equal to 231 GPa and Poisson's Ratio (v_f) equal to 0.2.
2. The composite laminate is considered to be transversely isotropic, i.e. a material with physical properties which are symmetric about an axis [14].
3. There is a perfect bonding between the matrix and the fibers [14].
4. The experimentally calculated volume fraction is accurate.
5. The fibers are properly aligned.
6. The interfacial effect between the fibers and matrix is negligible.

In our research the Rule of Mixture (ROM) is applied to evaluate the effective complex longitudinal modulus (E_1^*) and the effective in-plane Poisson's Ratio (v_{12}^*).

$$E_1^* = V_f E_f + V_m E_m^*$$
(63)

$$\nu_{12}^* = V_f \nu_f + V_m \nu_m^*$$
(64)

where V_f is the fiber volume fraction and V_m is the matrix volume fraction and E_m is determined experimentally as discussed in Section 3.3.

In the determination of the modulus in the direction transverse to the fibers and the in-plane shear modulus, the most commonly used model to predict the transverse modulus is the Inverse Rule of Mixture (IROM) as discussed in chapter 2. But a better prediction can be obtained with other various semi-emperical formulae such as Halpin Tsai, Cylindrical Assembly Model (CAM) and the Periodic Microstructure Model(PMM). In our research work, we select the Halpin Tsai Model because it is a flexible model with a curve fitting parameter, which is a measure of

reinforcement of the matrix by the fibers. It is also the only emperical model that also takes into consideration the environmental factors which affect the structural performance of composite materials [31]. i.e.

$$E_2^* = E_m^* \left[\frac{1 + \xi \eta V_f}{1 - \eta V_f} \right] \tag{65}$$

$$\eta = \frac{(E_f/E_m^*) - 1}{(E_f/E_m^*) + \xi} \tag{66}$$

where E_2^* is the complex transverse modulus, ζ is the curve fitting parameter which is also the measure of reinforcement of the matrix by the fibers.

And,

$$G_{12}^* = G_m^* \left[\frac{1 + \xi \eta V_f}{1 - \eta V_f} \right] \tag{67}$$

$$\eta = \frac{(G_f/G_m^*) - 1}{(G_f/G_m^*) + \xi} \tag{68}$$

where, G_{12}^* is the in-plane complex shear modulus and ζ is an emperical parameter obtained by curve fitting with the results of an analytical solution. A value of $\zeta = 2$ or 3 usually gives a good fit for the case of circular or square fibers.

Figure 48(a), 48(b) and 48(c) respectively shows the analytical results of viscoelastic properties of the in-plane longitudinal, the transverse and the in-plane shear moduli (storage and loss) versus reduced frequency. The analysis is conducted using a MATLAB code written based on the classical lamination theory (as discussed in Chapter 2), and can be found in Appendix A. Notice that E' and E'' for the longitudinal elastic moduli are almost constant, since the properties are dominated by the carbon fibers, which are assumed to be constant.

(a)

(b)

(c)

Figure.48: Plot of in-plane viscoelastic properties of the carbon/polyurethane lamina vs reduced frequency (a) Longitudinal modulus (E_1) (b) Transverse modulus (E_2) (c) In-plane shear modulus (G_{12}) vs Frequency.

The predicted analytical results of the in-plane transverse and in-plane shear complex moduli (storage and loss) for different methods (Halpin-Tsai, Tsai-Hahn, CAM and Inverse Rule of Mixture) for the transverse modulus and (Halpin-Tsai, CAM and PMM) for the shear modulus are displayed in Figures 49a and 49b respectively. The analysis is conducted using a MATLAB code written based on the classical lamination theory and different analytical models (as discussed in Chapter 2) and can be found in Appendix A.

(a)

(b)

Figure.49: Plot comparing the material properties using different analytical models (a) Complex transverse modulus (E_2) (b) In-plane complex shear modulus (G_{12}) vs Frequency.

The method that fits the corresponding experimental results the best is chosen. The Halpin–Tsai with $\zeta=3$ is chosen for predicting the in-plane transverse modulus and with $\zeta=2$ for the evaluation of the in-plane shear modulus. The comparison between the experimental and analytical results of the transverse and in-plane shear modulus are shown in Figures 50(a) and 50(b) respectively.

(a)

(b)

Figure.50: Plot comparing the experimental and analytical results (a) Complex transverse modulus (E$_2$) (b) In-plane complex shear (G$_{12}$) modulus vs Frequency.

A comparison between analytical and experimental results of the loss tangent for the transverse and in-plane shear modulus are shown in Figures 51(a) and 51(b).

(a)

(b)

Figure.51: Plot comparing the experimental and analytical results of the loss tangent values (a) Complex transverse modulus (E_2) (b) In-plane complex shear (G_{12}) modulus vs Frequency.

4.2. Viscoelastic Properties of a 3-Layer Carbon-Polyurethane (C/PU) Laminate.

After finding the complex transverse (E_2) and in-plane shear (G_{12}) moduli of a carbon-polyurethane lamina using different analytical models and comparing it with the experimental results, the next step is to determine the material properties of a sample 3-layer laminate. A sample laminate with orientation angles [θ/β/θ] similar to the laminate structure used by Ghoneim and Zhen [2] in the FMC pump was used. Preliminary analysis was conducted to determine the laminate modulus of the 3-layer laminate.

A set of equivalent laminate moduli E_x, E_y, G_{xy} and E_b can be defined for symmetric laminates. These moduli represent the stiffness of a fictitious, equivalent, orthotropic plate that behaves like the actual laminate under in-plane loads. It should be pointed out that the same laminates presented in Table. 4 are analytically studied. The analysis was done using MATLAB, and the code can be found in Appendix A. Figure 52 shows the analytical laminate moduli vs frequency; i.e. the complex extensional modulus (E_x) in x-direction for the two different laminates (Figure 52a), the complex extensional modulus (E_y) in y-direction (Figure 52b), the complex in-plane shear modulus (G_{xy}) for the two different laminates (Figure 52c) and the bending modulus (E_b) (Figure 52d) vs. the reduced frequency.

(a)

(b)

(c)

(d)

Figure.52: Plot of laminate moduli vs reduced frequency (a) Extensional modulus (E_x) (b) Extensional Modulus (E_y) (c) Shear modulus (G_{xy}) (d) Extensional bending modulus (E_b) vs Frequency.

Based on the experiments conducted in Section 3.4, Figure 53 shows the comparison between the experimental and analytical laminate moduli vs frequency, i.e., the complex extensional (E_x) in x-direction (Figure 53a), the complex extensional (E_y) in y-direction (Figure 53b), the complex in-plane shear (G_{xy}) modulus (Figure 53c) and the bending (E_b) modulus (Figure 53d) vs the reduced frequency.

(a)

Extensional Modulus [Ey] vs Reduced Frequency

(b)

Laminate Shear Modulus [Gxy] vs Reduced Frequency

(c)

(d)

Figure.53: Plot comparing the experimental and theoretical results (a) Laminate elastic modulus (E_x) (b) Laminate elastic modulus (E_y) (c) Laminate shear modulus (G_{xy}) (d) Laminate bending modulus (E_b) vs Frequency.

Figure 54 shows the comparison between analytical and experimental results of the loss tangent for different laminate moduli, i.e., the complex extensional (E_x) in x-direction (Figure 54a), the complex extensional (E_y) in y-direction (Figure 54b), the complex in-plane shear (G_{xy}) modulus (Figure 54c) and the bending (E_b) modulus (Figure 54d) vs the reduced frequency.

(a)

Comparing the Experimental & Analytical Loss Tangent [Tan(d)] for Extensional Modulus (Ey)

(b)

Comparing the Experimental & Analytical Loss Tangent [Tan(d)] for Shear Modulus (Gxy)

(c)

(d)

Figure.54: Plot comparing the experimental and theoretical results for the loss tangent values (a) Laminate elastic modulus (E_x) (b) Laminate elastic modulus (E_y) (c) Laminate shear modulus (G_{xy}) (d) Laminate bending modulus (E_b) vs Frequency.

In general, though the predicted analytical results of the storage moduli underestimate the corresponding experimental one. The loss tangent (Tan(δ)) results are reasonable within the targeted range of study.

4.3. Effective Damping of a 3-Layer Carbon-Polyurethane (C/PU) Laminate

After finding the laminate moduli and comparing it with the experimental results, the next step is to use the correspondence principle in combination with the Adams and Bacon method (as discussed in chapter 2) to evaluate the overall effective damping of the laminate structure. This depends on the type of loading. In the current work, uniaxial loading and shear loading is being investigated. In general the effective damping (η) is given by

$$\eta = \frac{W^d}{W^e} = \frac{\sum_k W_k^d}{\sum_k W_k^e}$$

(69)

where W^e is the total elastic strain energy per cycle of loading, W^d is the total dissipated energy per cycle, and k is the layer (lamina) number. If W is the total work done per cycle, then

$$W = \sum_k W_k = \sum_k (W_k^e + W_k^d)$$

$$= \sum_k \int \sigma_k \epsilon_k dV$$

$$= \sum_k \frac{1}{2} \int \sigma_T^k [S^*]_k \sigma_k dV$$

(70)

where σ_k and ε_k are the in-plane stress and strain vectors in the material co-ordinates for lamina k and $[S_k^*]$ = inv $[Q_k^*]$ is the reduced in-plane compliance matrix as discussed in Chapter 2. For a specific kind of loading (axial and shear), the stress and the strain vectors in the global coordinates are determined. These stress and strain vectors are used to determine the stress and strain vectors in the material coordinates, which in turn is used to calculate the work done and damping factor as shown in equations (69) and (70).

In our research work, the effective extensional damping factor (due to uniaxial loading) and shear damping factor (due to pure shear loading) are evaluated for the 3-layer [θ/β/θ] laminate structure as functions of the two angles θ and β. The results are presented next. All results presented next are purely analytical. The analysis was done using MATLAB and the code can be found in Appendix A.

Figure. 55 shows the color map plot of the effective axial (extensional) damping factor as a function of the two angles θ and β of the 3-layer laminate at two frequencies of 1Hz (Figure 55a) and 10Hz (Figure 55b). It is clear that at 1 Hz a high damping factor of more than 0.11 can be found at a wide range of θ and β, whereas at 10 Hz a higher damping factor of more than 0.12 can be found at the same range. So in general, since a higher damping is preferred for vibration isolation application (in order to dissipate more of the excessive energy of vibration), high damping can be easily achieved under uniaxial loading of the 3-layer laminate. But, on the other hand low damping is confined to a very narrow region which is difficult to achieve. Consequently, this is not suitable to be used for pumping applications.

(a)

(b)

Figure.55: Plot of axial damping factor vs laminate angles (a) Axial damping factor at 1Hz (b) Axial damping factor at 10Hz vs Laminate angles.

Similarly, Figure. 56 shows the color map plot of the effective shear damping factor as a function of the two angles θ and β of the 3-layer laminate at two frequencies of 1Hz (Figure 56a) and 10Hz (Figure 56b). It is clear that at 1 Hz a high damping factor of more than 0.11 can be found at a wide range of θ and β, whereas at 10 Hz a higher damping factor of more than 0.12 can be found at the same range of θ and β [which roughly ranges between (θ=20^0–90^0 and β= 20^0-90^0)].

(a)

(b)

Figure.56: Plot of shear damping factor vs laminate angles (a) Shear damping factor at 1Hz (b) Shear damping factor at 10Hz vs Laminate angles.

Taking a closer look (zooming in) at the color-map plots of the effective axial and shear loss factors is displayed in Figures 57 (a & b) and 58 (a & b), respectively. They reveal that there exists a very tight area of high effective loss factor in the vicinity of θ=β (any slight deviation from θ= β renders a huge change in η). This range is very impractical since it is too tight to be achieved.

(a)

(b)

Figure.57: A zoom in plot of axial damping factor vs laminate angles (a) Axial damping factor at 1Hz (b) Axial damping factor at 10Hz vs Laminate angles.

Figure.58: A zoom in plot of shear damping factor vs laminate angles (a) Shear damping factor at 1Hz (b) Shear damping factor at 10Hz vs Laminate angles.

According to Ghoneim and Yin [2], the high negative effective Poisson's ratio values are confined to a very tight zone. This tight zone occurs in the vicinity of $\theta = 0^0$ - 5^0 and $\beta = 10^0 - 50^0$, which requires a very precise fiber lay-up technique to manufacture. This zone, in general, is characterized by a high effective axial (extensional) and shear loss factor, as shown in Figures 59

and 60 respectively. Consequently, the problem of selecting the proper fiber-angle orientation may be a trade-off problem between the high negative Poisson's ratio, which contributes to increasing the volumetric efficiency, and the low damping factor required to achieve a high power efficiency.

(a)

(b)

Figure 59: Zoom in plot of the effective axial loss factor (a) at 1Hz (b) at 10Hz.

Figure 60: Zoom in plot of the effective shear loss factor (a) at 1Hz (b) at 10Hz.

Chapter 5

Conclusions and Future Work

The viscoelastic material characteristics of Polyurethane (PU) were found using the Dynamic Mechanical Analyzer (DMA). Assuming that the carbon fiber is purely elastic, the in-plane viscoelastic properties such as longitudinal (E_1), transverse (E_2) and shear (G_{12}) moduli were computed using the correspondence principle along with the micromechanics approach. Since the longitudinal modulus (E_1) is a fiber dominated property, only transverse (E_2) and in-plane shear (G_{12}) moduli were tested using the DMA. A fair agreement in the moduli are found between the experimental results and the analytical prediction. Applying the Classical Lamination Theory (CLT), the laminate moduli (E_x, E_y, G_{xy} and E_b) were calculated and compared with the corresponding experimental results for two different laminates ([5/35/5] and [30/-60/30]). A fair agreement in the moduli between the experiments and the analytical prediction was found. The differences in the results can be attributed to the following:

- Imperfect test specimens. Though care has been exercised upon the preparation and manufacturing of the laminates, they are being prepared manually, which may render inconsistent thickness and fiber angle orientation.
- Use of a different batches of PU for the laminate, which may have a slightly different viscoelastic properties.
- The assumptions which are employed, as discussed in Section 4.1, for the analytical evaluation of the viscoelastic properties of the carbon/PU laminae (Rule of mixture and Tsai-Hahn assumptions).
- The difficulty in determining the shear modulus experimentally. The optimum pressure needed to prevent the shear sample from slipping without affecting the applied shearing poses major challenge.

By applying the Adams Bacon criteria, the effective axial (extensional) and shear loss factors of the 3-layer laminate [θ/β/θ] were realized as functions of the two angles θ and β. The results were compared with the corresponding results of the effective Poison's Ratio provided by Ghoneim and Yin [6]. No clear correlation between the damping factor and Poisson's Ratio are found. The high pumping potential (PP) of the [5/35/5] laminate, with a negative effective Poisson's Ratio as proposed by Ghoneim and Yin [6], has an inherent high damping and is not suitable for the novel pump proposed. However, the arrangement may be appropriate for vibration isolation applications.

The recommended future work includes:
1. Apply a more accurate method (manufacturing process) for preparing the laminates, for example, the composite 3-D printer; which renders a more accurate volume fraction and orientation angles and a better inter laminar bonding.

2. Investigate the relationship between the damping factors under combined loading and the effective negative Poison's ratio.
3. Investigate the applications of different types of FMC materials on the damping factors.

Chapter 6
Bibliography

1. J.D.Inman, "Engineering Vibration", Prentice Hall Inc., New Jersey, 2001, pp 399-400.
2. J.Nawroth, J.Dabiri, Fluid Transport in Muscular Pumps at Intermediate Reynolds Numbers, 63rd Annual Meeting of American Physical Society, Division of Fluid Dynamics, Long Beach, CA 2010; Vol 55(16).
3. A. Chanda, H. Ghoneim, Pumping potential of a two-layer left-ventricle-like flexible-matrix-composite structure. Composite Structures, 2015, pp. 570-575.
4. A. Lotfi-Gaskarimahalle, L.H. Scarborough III, C.D. Rahn, and E.C. Smith, Tunable fluidic composite mounts for vibration absorber. Journal of Vibration and Control, Vol. 4, 2014, pp. 2137 - 2145.
5. R.S. Gureghian, J.D. Carlson, D.F LeRoy, R.H. Marjoram, M.B. Brown, M.R. Jolly, Controllable platform suspension system for treadmill decks and like devices therefor. Patent US 5993358 A, Nov. 1999.
6. Z. Yin, and H. Ghoneim, Pumping Potential of a Flexible Matrix Composite Structure with Negative Poisson's Ratio. Abstracts of First International Conference on Mechanics of Composites, Stony Brook University, Long Island, NY, June 9-12, 2014.
7. Dynamic Mechanical Analysis Basics: Part 1 How DMA Works, Technical Note, Thermal Analysis, www.perkinselmer.com, 2007
8. Y.Shan and Bakis C.E Viscoelastic Characterization and Self-Heating Behavior of a Flexible Matrix Composite Drive Shaft, Journal of Composite Materials 2009 43: 1335.
9. Dynamic Mechanical Analysis, A Beginner's Guide, www.perkinselmer.com, 2008.
10. Kevin P.Menard…. Dynamic Mechanical Analysis - A Practical Introduction (2nd Edition), 2008, ISBN 978-1-4200-5312-8.
11. http://commons.wikimedia.org/wiki/File:Schematic_of_DMA.png
12. J.D.D Melo, and D.W. Radford, Viscoelastic characterization of transversely isotropic composite laminates. Journal of Composite Materials, 2003, Vol. 37 (2).
13. John D. Ferry, Viscoelastic Properties of Polymers (3rd Edition), Wiley, New York, 1980.
14. Neil MacAloney, Andres Bujanda, Robert Jensen, and Nakhiah Goulbourne, Viscoelastic Characterization of Aliphatic Polyurethane Interlayers, October 2009.
15. Melo J.D.D., and Radford D.W., Time and Temperature Dependence of the Viscoelastic propertied of PEEK/IM7. Journal of Composite Materials, Vol. 38 (20), 2004.
16. R.Chandra, S.P Singh, K.Gupta, Damping Studies in Fiber-Reinforced Composites-A Review, Composite Structures 46(1999) 41-51.
17. Suarez SA, Gibson RF, Sun CT, Chaturvedi SK. The Influence of Fiber Length and Fiber Orientation on Damping and Stiffness of Polymer Composite Materials. 1986.
18. E. J. Barbero, Introduction to composite materials design, CRC Press, Taylor & Francis Group, 2011. ISBNb978-1-4200-7915-9.
19. R. E. Swain, K. L. Reifsnider, K. Jayaraman and M.El-Zein, Interface/Interphase Concepts in Composite Material Systems, Journal of THERMOPLASTIC COMPOSITE MATERIALS, Vol. 3 -January 1990.

20. Keshavamurthy. D, Hossakere K. M., and Peel L. D., Vibration Damping of Fiber-Reinforced Polyurethane using High and Negative Poisson's Ratio Laminates. SAMPE Conference Proceedings 2005.

21. R.D. Adams, and D.G.C. Bacon, Effect of fiber orientation and laminate geometry on the dynamic properties of CFRP, Journal of Composite Materials, 1973, Vol. 7.

22. Y.J. Chen, F. Scarpa, I.R. Farrow, T.J. Liu, and J.S. Leng. Composite flexible skin with large negative Poisson's Ratio range: numerical and experimental analysis. Smart Materials and Structures, 22:045005, 2013.

23. K. Fukushima, H. CAI, M. Nakada, and Y. Miyano, Determination of time-temperature shift factor for long-term life prediction of polymer composites. ICCM-17, 17th International Conference on Composite Materials, 2009.

24. Alexander RASA, Applying Dynamic Mechanical Analysis to Research & Development for Viscoelastic Damping Materials, Inter-Noise 2014.

25. A. Katunin, W. Hufenbach, K. Holeczek, Frequency Dependence of the Self-Heating Effect in Polymer-based Composites, Journal of Achievements in Materials and Manufacturing Engineering, Vol 41-Issue 1-2, 2010.

26. C.P.Chen and R.S.Lakes, Analysis of High Loss Viscoelastic Composites, Journal of Material Science, Vol 28, 4229-4304, 1993.

27. Z.Hashin, Complex Moduli of Viscoelastic Composites-II Fiber Reinforced Materials, International Journal of Solids and Structures, 1970, Vol 6, pp.797-807.

28. N. Kumar, B. Varela, and H. Ghoneim, Effective damping of a flexible-matrix-composite laminate with a negative effective Poisson's ratio. Proceedings of the ASME 2015 International Mechanical Engineering Congress and Exposition, IMECE2015-50365, November 13-19, 2015, Houston, Texas USA.

29. Andrey V. Boiko, Victor M. Kulik, Basel M. Seoudi, H.H. Chun, Inwon Leed, Measurement Method of Complex Viscoelastic Material Properties, International Journal of Solids and Structures, Vol 47, Issues 3-4, February 2010, Pages 374-382.

30. N.W.Tscoegl, Wolfgang G.Knauss and Igor Emri, Poisson's Ratio in Linear Viscoelasticity –A Critical Review, Mechanics of Time Dependent Materials 6: 3-51,2002.

31. J.C.Halpin and S.W.Tsai, Effects of Environmental Factors on Composite Materials, Technical Report AFML-TR-67-423, Airforce Materials Laboratory.

Chapter 7
Appendix
Appendix A

Code Listing

A.1. MATLAB Codes for Composite Laminates
A.1.1. Function calculating the volume fraction of matrix and fiber

```
clc
clear all
%Calculation of Volume Fractions%
%wf - Weight of Fiber in Kg%
wf=25.515e-3;
%wc - Weight of Composite in Kg%
wc=60.91e-3;
%wm - Weight of Matix in Kg%
wm=wc-wf;
%Wf - Fiber Weight Fraction%
Wf=wf/wc;
%Wm - Matrix Weight Fraction%
Wm=wm/wc;
%pf - Density of Fiber in Kg/m3%
pf=1750;
%pm - Density of Matrix in Kg/m3%
pm=1200;
%pc - Density of Composite%
pc=(pm*pf)/((Wf*pm)+(Wm*pf));
%Vf - Volume Fraction of Fiber %
Vf=(Wf*pc)/pf;
%Vm - Volume Fraction of Matrix%
Vm=(Wm*pc)/pm;
```

A.1.2. Function for calculating the in-plane properties of the lamina

```
clc
clear all
close all
%%%%%%%%%%%%%%%%%%%%%%%%%%%%%%%%%%%%%%%%%%%%%%%%%%%%%%%%%%%%%%%%%%%%%%%%%%
%%%%%
%Calculation of Volume Fractions%
%wf - Weight of Fiber in Kg%
wf=25.515e-3;
%wc - Weight of Composite in Kg%
wc=60.91e-3;
%wm - Weight of Matix in Kg%
wm=wc-wf;
%Wf - Fiber Weight Fraction%
Wf=wf/wc;
%Wm - Matrix Weight Fraction%
Wm=wm/wc;
%pf - Density of Fiber in Kg/m3%
```

```matlab
pf=1750;
%pm - Density of Matrix in Kg/m3%
pm=1200;
%pc - Density of Composite%
pc=(pm*pf)/((Wf*pm)+(Wm*pf));
%Vf - Volume Fraction of Fiber %
Vf=(Wf*pc)/pf;
%Vm - Volume Fraction of Matrix%
Vm=(Wm*pc)/pm;
%%%%%%%%%%%%%%%%%%%%%%%%%%%%%%%%%%%%%%%%%%%%%%%%%%%%%%%%%%%%%%%%%%%%%%
%%%%%
%Modulus is in the form of the Equation, E = a2*x^2 + a1*x + a0%
%Where, x= log(at*w) is the Reduced Frequency%=288
%Properties of Polyurethane%
a21 = 97.611e3; a11 = 31.112e3; a01 = 965.287e3;
a22 = 71.511e3; a12 = -30.415e3; a02 = 111.848e3;
b21 = 15.494e3; b11 = 24.085e3; b01 = 259.327e3;
b22 = 13.629e3; b12 = -0.84646e3; b02 = 26.003e3;
w=1:1:100; %Reference Frequency in Hz%
T0=288; %Reference Temperature in Kelvin%
C1e=0.47;  %Shift Factor Constants%
C2e= 43.36; %Shift Factor Constants%
C1g=0.53; %Shift Factor Constants%
C2g=46.45; %Shift Factor Constants%
% For Reference Temperature of 15C or 288K%
T=288;
%calculation of Shift Factor%
Xe=(-C1e*(T-T0))/(C2e+(T-T0));
Xg=(-C1g*(T-T0))/(C2g+(T-T0));
Ate=10^Xe;          %Shift Factor of Elastic Modulus%
Atg=10^Xg;          %Shift Factor of Shear Modulus%
xe=log10(Ate*w);
xg=log10(Atg*w);
Eprime=(a21*xe.^2)+(a11*xe)+a01;    %Elastic Storage Modulus of Poly-
Urethane in KPA%
Edprime=(a22*xe.^2)+(a12*xe)+a02;   %Elastic Loss Modulus of
Polyurethane in KPA%
Gprime= (b21*xg.^2)+(b11*xg)+b01;   %Shear Storage Modulus of
Polyurethane in KPA%
Gdprime=(b22*xg.^2)+(b12*xg)+b02;   %Shear Loss Modulus of
Polyurethane in KPA%
Em=Eprime+Edprime*i;            %Extentional Modulus(Complex) of
Polyurethane in KPA%
Gm=Gprime+Gdprime*i;            %Shear Modulus(Complex) of
Polyurethane in KPA %
vm=(Em)/(2*Gm)-1;           %Poisson's Ratio(Complex) of Polyurethane%
%%%%%%%%%%%%%%%%%%%%%%%%%%%%%%%%%%%%%%%%%%%%%%%%%%%%%%%%%%%%%%%%%%%%%%
%%%%%
%Properties of Carbon Fiber%
Ef=231*10^9;                    %Elastic Modulus of Carbon Fiber in
KPA%
vf=0.2;                         %Poisson's Ratio of Carbon Fiber%
```

```matlab
Gf=Ef/(2*(1+vf));                    % Shear Modulus of Carbon Fiber%
%%%%%%%%%%%%%%%%%%%%%%%%%%%%%%%%%%%%%%%%%%%%%%%%%%%%%%%%%%%%%%%%%%%%%%%%
%%%%%
%Properties of the Lamina(Carbon-PolyUrethane)%
Vf= 0.3308;
Vm=0.6692;
%%%%%%%%%%%%%%%%%%%%%%%%%%%%%%%%%%%%%%%%%%%%%%%%%%%%%%%%%%%%%%%%%%%%%%%%
%%%%%
%Longitudinal Modulus (E1) Calculated using Different Models%
%Using Rule of Mixture%
E1=(Ef*Vf)+(Em*Vm);
%%%%%%%%%%%%%%%%%%%%%%%%%
%Seperating Real and Imaginary Values%
E1r=real(E1);
E1i=imag(E1);
%%%%%%%%%%%%%%%%%%%%%%%
figure
loglog(w,E1r,'*b')
hold on
loglog(w,E1i,'*r')
hold off
grid on
xlabel('Log Frequency(Hz)')
ylabel ('Longitudinal Modulus [E1] (Pa)')
legend ( 'Storage Modulus','Loss Modulus')
title('Longitudinal Modulus [E1] vs Frequency')
%%%%%%%%%%%%%%%%%%%%%%%%%%%%%%%%%%%%%%%%%%%%%%%%%%%%%%%%%%%%%%%%%%%%%%%%
%%%%%
%In Plane Poisson's Ratio Calculated using Different Models%
%Using Rule of Mixture%
v12=(vf*Vf)+(vm*Vm);
%Seperating Real and Imaginary Parts%
v12r=real(v12);
v12i=imag(v12);
%%%%%%%%%ROM%%%%%%%%%%%
figure
loglog(w,v12r,'*b')
hold on
loglog(w,v12i,'*r')
hold on
grid on
xlabel('Log Frequency(Hz)')
ylabel ('In-plane Poissons Ratio [v12] ')
title('In-plane Poissons Ratio [v12] vs Frequency')
%%%%%%%%%%%%%%%%%%%%%%%%%%%%%%%%%%%%%%%%%%%%%%%%%%%%%%%%%%%%%%%%%%%%%%%%
%%%%%
%Transverse Modulus (E2) Calculated Using Different Emperical models%
%Using Halpin-Tsai%
Z= 2;                            %Curve Fitting Parameter%
n = ((Ef./Em)-1)./((Ef./Em)+Z);
E2= Em.*((1+Z*n*Vf)./(1-n*Vf));
%Seperating Real and Imaginary Parts%
```

```
E2r=real(E2);
E2i=imag(E2);
%%%%%%%%Halpin-Tsai%%%%%%%%%%
figure
loglog(w,E2r,'*b')
hold on
loglog(w,E2i,'*r')
hold on
grid on
xlabel('Log Frequency(Hz)')
ylabel ('Transverse Modulus [E2] (Pa)')
legend ( 'Storage Modulus','Loss Modulus')
title('Transverse Modulus [E2] vs Frequency')
%%%%%%%%%%%%%%%%%%%%%%%%%%%%%%%%%%%%%%%%%%%%%%%%%%%%%%%%%%%%%%%%%%%%%%%%%
%%%%%
%Shear Modulus Calculated Using Different Emperical Models%
%Using Halpin-Tsai%
Z= 2;                           %Curve Fitting Parameter%
n = ((Gf./Gm)-1)./((Gf./Gm)+Z);
G12= Gm.*((1+Z*n*Vf)./(1-n*Vf));
%Seperating Real and Imaginary Parts%
G12r=real(G12);
G12i=imag(G12);
%%plot%%
figure
loglog(w,G12r,'*b')
hold on
loglog(w,G12i,'*r')
hold on
grid on
xlabel('Log Frequency(Hz)')
ylabel ('Shear Modulus[G12](Pa)')
legend ( 'Storage Modulus','Loss Modulus')
title('Shear Modulus[G12] vs Frequency')
```

A.1.3. Function for comparing the in-plane properties of the lamina

```
clear all
clc
close all
%%%%%%%%%%%%%%%%%%%%%%%%%%%%%%%%%%%%%%%%%%%%%%%%%%%%%%%%%%%%%%%%%%%%%%%%%
%%%%%
%Calculation of Volume Fractions%
%wf - Weight of Fiber in Kg%
wf=25.515e-3;
%wc - Weight of Composite in Kg%
wc=60.91e-3;
%wm - Weight of Matix in Kg%
wm=wc-wf;
%Wf - Fiber Weight Fraction%
Wf=wf/wc;
%Wm - Matrix Weight Fraction%
```

```matlab
Wm=wm/wc;
%pf - Density of Fiber in Kg/m3%
pf=1750;
%pm - Density of Matrix in Kg/m3%
pm=1200;
%pc - Density of Composite%
pc=(pm*pf)/((Wf*pm)+(Wm*pf));
%Vf - Volume Fraction of Fiber %
Vf=(Wf*pc)/pf
%Vm - Volume Fraction of Matrix%
Vm=(Wm*pc)/pm
%%%%%%%%%%%%%%%%%%%%%%%%%%%%%%%%%%%%%%%%%%%%%%%%%%%%%%%%%%%%%%%%%%%%%%%%%
%%%%%
%Modulus is in the form of the Equation, E = a2*x^2 + a1*x + a0%
%Where, x= log(at*w) is the Reduced Frequency%=288
%Properties of Polyurethane%
a21 = 97.611e3; a11 = 31.112e3; a01 = 965.287e3;
a22 = 71.511e3; a12 = -30.415e3; a02 = 111.848e3;
b21 = 15.494e3; b11 = 24.085e3; b01 = 259.327e3;
b22 = 13.629e3; b12 = -0.84646e3; b02 = 26.003e3;
w=1:1:100; %Reference Frequency in Hz%
T0=288; %Reference Temperature in Kelvin%
C1e=0.47;  %Shift Factor Constants%
C2e= 43.36; %Shift Factor Constants%
C1g=0.53; %Shift Factor Constants%
C2g=46.45; %Shift Factor Constants%
% For Reference Temperature of 15C or 288K%
T=288;
%calculation of Shift Factor%
Xe=(-C1e*(T-T0))/(C2e+(T-T0));
Xg=(-C1g*(T-T0))/(C2g+(T-T0));
Ate=10^Xe;         %Shift Factor of Elastic Modulus%
Atg=10^Xg;         %Shift Factor of Shear Modulus%
xe=log10(Ate*w);
xg=log10(Atg*w);
Eprime=(a21*xe.^2)+(a11*xe)+a01;    %Elastic Storage Modulus of Poly-
Urethane in KPA%
Edprime=(a22*xe.^2)+(a12*xe)+a02;   %Elastic Loss Modulus of
Polyurethane in KPA%
Gprime= (b21*xg.^2)+(b11*xg)+b01;   %Shear Storage Modulus of
Polyurethane in KPA%
Gdprime=(b22*xg.^2)+(b12*xg)+b02;   %Shear Loss Modulus of
Polyurethane in KPA%
Em=Eprime+Edprime*i;               %Extentional Modulus(Complex) of
Polyurethane in KPA%
Gm=Gprime+Gdprime*i;               %Shear Modulus(Complex) of
Polyurethane in KPA %
vm=(Em)/(2*Gm)-1          %Poisson's Ratio(Complex) of Polyurethane%
%%%%%%%%%%%%%%%%%%%%%%%%%%%%%%%%%%%%%%%%%%%%%%%%%%%%%%%%%%%%%%%%%%%%%%%%%
%%%%%
%Properties of Carbon Fiber%
```

```matlab
Ef=231*10^9;                        %Elastic Modulus of Carbon Fiber in
KPA%
vf=0.2;                             %Poisson's Ratio of Carbon Fiber%
Gf=Ef/(2*(1+vf));                   % Shear Modulus of Carbon Fiber%
%%%%%%%%%%%%%%%%%%%%%%%%%%%%%%%%%%%%%%%%%%%%%%%%%%%%%%%%%%%%%%%%%%%%%%%%%
%%%%%
%Properties of the Lamina(Carbon-PolyUrethane)%
Vf= 0.3308;
Vm=0.6692;
%%%%%%%%%%%%%%%%%%%%%%%%%%%%%%%%%%%%%%%%%%%%%%%%%%%%%%%%%%%%%%%%%%%%%%%%%
%%%%%
%Longitudinal Modulus (E1) Calculated using Different Models%
%Using Rule of Mixture%
E1=(Ef*Vf)+(Em*Vm);
%%%%%%%%%%%%%%%%%%%%%%%%%
%Seperating Real and Imaginary Values%
E1r=real(E1);
E1i=imag(E1);
%%%%%%%%%%%%%%%%%%%%%%%
figure
loglog(w,E1r,'*b')
hold on
loglog(w,E1i,'*r')
hold off
grid on
xlabel('Log Frequency(Hz)')
ylabel ('Longitudinal Modulus [E1] (Pa)')
legend ( 'Storage Modulus','Loss Modulus')
title('Longitudinal Modulus [E1] vs Frequency')
%%%%%%%%%%%%%%%%%%%%%%%%%%%%%%%%%%%%%%%%%%%%%%%%%%%%%%%%%%%%%%%%%%%%%%%%%
%%%%%
%In Plane Poisson's Ratio Calculated using Different Models%
%Using Rule of Mixture%
v12=(vf*Vf)+(vm*Vm);
%%%%%%%%%%%%%%%%%%%%%%%%%%%%%%%%%%%%%%%%%%%%%%%%%%%%%%%%%%%%%%%%%%%%%%%%%
%%%%%
%Transverse Modulus (E2) Calculated Using Different Emperical models%
%Using Halpin-Tsai%
Z= 3;                               %Curve Fitting Parameter%
n = ((Ef./Em)-1)./((Ef./Em)+Z);
E2H= Em.*((1+Z*n*Vf)./(1-n*Vf));
%Using Tsai-Hahn%
n=1;                                %Stress Partitioning Parameter%
E2T = (1/(Vf+n*Vm)*((Vf./Ef)+n*(Vm./Em))).^-1;
%Using Matrix Dominated Cylindrical Assembly Model (CAM)%
E2C= Em *((1+Vf)/(1-Vf));
%Using Inverse Rule of Mixture%
Z= 0;                               %Curve Fitting Parameter%
n = ((Ef./Em)-1)./((Ef./Em)+Z);
E2I= Em.*((1+Z*n*Vf)./(1-n*Vf));
%Seperating Real and Imaginary Parts%
E2Hr=real(E2H);
```

```
E2Hi=imag(E2H);
E2Tr=real(E2T);
E2Ti=imag(E2T);
E2Cr=real(E2C);
E2Ci=imag(E2C);
E2Ir=real(E2I);
E2Ii=imag(E2I);
%%%%%%%%%Halpin-Tsai%%%%%%%%%%%
figure
loglog(w,E2Hr,'*b')
hold on
loglog(w,E2Hi,'*r')
hold on
grid on
xlabel('Log Frequency(Hz)')
ylabel ('Transverse Modulus [E2] (Pa)')
legend ( 'Storage Modulus','Loss Modulus')
title('Transverse Modulus [E2] vs Frequency (Halpin Tsai)')
%%%%%%%Tsai-Hahn%%%%%%%%%%
figure
loglog(w,E2Tr,'*b')
hold on
loglog(w,E2Ti,'*r')
hold off
grid on
xlabel('Log Frequency(Hz)')
ylabel ('Transverse Modulus [E2] (GPa)')
legend ( 'Storage Modulus','Loss Modulus')
title('Transverse Modulus [E2] vs Frequency (Tsai-Hahn)')
%%%%%%%%%CAM%%%%%%%%%%%%%
figure
loglog(w,E2Cr,'*b')
hold on
loglog(w,E2Ci,'*r')
hold off
grid on
xlabel('Log Frequency(Hz)')
ylabel ('Transverse Modulus [E2] (Pa)')
legend ( 'Storage Modulus','Loss Modulus')
title('Transverse Modulus [E2] vs Frequency (CAM)')
%%%%%Inverse Rule of Mixture%%%%%%%%%%%%
figure
loglog(w,E2Ir,'*b')
hold on
loglog(w,E2Ii,'*r')
hold off
grid on
xlabel('Log Frequency(Hz)')
ylabel ('Transverse Modulus [E2] (Pa)')
legend ( 'Storage Modulus','Loss Modulus')
title('Transverse Modulus [E2] vs Frequency (IROM)')
```

```matlab
%%%%%%%%%%%%%%%%%%%%%%%%%%%%%%%%%%%%%%%%%%%%%%%%%%%%%%%%%%%%%%%%%%%%%%%%%
%%%%%
%Shear Modulus Calculated Using Different Emperical Models%
%Using Halpin-Tsai%
Z= 2;                              %Curve Fitting Parameter%
n = ((Gf./Gm)-1)./((Gf./Gm)+Z);
G12H= Gm.*((1+Z*n*Vf)./(1-n*Vf));
%Using Periodic Micro structure Model (PMM)%
S3=0.49247-0.47603*Vf-0.02748*Vf^2;
G12P=Gm.*(1+((Vf*(1-Gm/Gf))/((Gm/Gf)+S3*(1-Gm/Gf))));
%Using Matrix Dominated Cylindrical Assembly Model (CAM)%
G12C= Gm.*((1+Vf)/(1-Vf));
%Seperating Real and Imaginary Parts%
G12Hr=real(G12H);
G12Hi=imag(G12H);
G12Pr=real(G12P);
G12Pi=imag(G12P);
G12Cr=real(G12C);
G12Ci=imag(G12C);
%%%%%%%%%Halpin-Tsai%%%%%%%%%%%
figure
loglog(w,G12Hr,'*b')
hold on
loglog(w,G12Hi,'*r')
hold on
grid on
xlabel('Log Frequency(Hz)')
ylabel ('Shear Modulus[G12](Pa)')
legend ( 'Storage Modulus','Loss Modulus')
title('Shear Modulus[G12] vs Frequency (Halpin Tsai)')
%%%%%%%Tsai-Hahn%%%%%%%%%%%
figure
loglog(w,G12Pr,'*b')
hold on
loglog(w,G12Pi,'*r')
hold off
grid on
xlabel('Log Frequency(Hz)')
ylabel ('Shear Modulus [G12] (Pa)')
legend ( 'Storage Modulus','Loss Modulus')
title('Shear Modulus [G12] vs Frequency (PMM)')
%%%%%%%%%CAM%%%%%%%%%%%%%
figure
loglog(w,G12Cr,'*b')
hold on
loglog(w,G12Ci,'*r')
hold off
grid on
xlabel('Log Frequency(Hz)')
ylabel ('Shear Modulus [G12] (Pa)')
legend ( 'Storage Modulus','Loss Modulus')
title('Shear Modulus [G12] vs Frequency (CAM)')
```

```
%%%%%%%%%%%%%%%%%%%%%%%%%%%%%%%%%%%%%%%%%%%%%%%%%%%%%%%%%%%%%
```

A.1.4. Function for calculating the properties of a laminate

```
clc
clear all
close all
thickness   = 2.36; %Thickness of the Laminate in mm%
nl          = 3;     %Number of Layers in the Laminate%
d = thickness/nl;
z = [-1.5*d, -0.5*d, 0.5*d, 1.5*d]; %Z-Vector of the Laminate%
thetav = [10, 40, 10];  %Orientation Angle Vector of the Laminate%
ii = 0;
for x = 0:0.1:2
ii = ii + 1;
A0 = zeros(3);
B0 = zeros(3);
D0 = zeros(3);
for j=1:3
thetd = thetav(j);
%%%%%%%%%%%%%%%%%%%%%%%%%%%%%%%%%%%%%%%%%%%%%%%%%%%%%%%%%%%%%%%%%%%%%%%%%%%%
%%%%%
%Calculation of Volume Fractions%
%wf - Weight of Fiber in Kg%
wf=25.515e-3;
%wc - Weight of Composite in Kg%
wc=60.91e-3;
%wm - Weight of Matix in Kg%
wm=wc-wf;
%Wf - Fiber Weight Fraction%
Wf=wf/wc;
%Wm - Matrix Weight Fraction%
Wm=wm/wc;
%pf - Density of Fiber in Kg/m3%
pf=1750;
%pm - Density of Matrix in Kg/m3%
pm=1200;
%pc - Density of Composite%
pc=(pm*pf)/((Wf*pm)+(Wm*pf));
%Vf - Volume Fraction of Fiber %
Vf=(Wf*pc)/pf;
%Vm - Volume Fraction of Matrix%
Vm=(Wm*pc)/pm;
%%%%%%%%%%%%%%%%%%%%%%%%%%%%%%%%%%%%%%%%%%%%%%%%%%%%%%%%%%%%%%%%%%%%%%%%%%%%
%%%%%
%Material Properties of Polyurethane (PU) Matrix%
a21 = 97.611e3; a11 = 31.112e3; a01 = 965.287e3;
a22 = 71.511e3; a12 = -30.415e3; a02 = 111.848e3;
b21 = 15.494e3; b11 = 24.085e3; b01 = 259.327e3;
b22 = 13.629e3; b12 = -0.84646e3; b02 = 26.003e3;
Eprime=(a21*x.^2)+(a11*x)+a01;    %Elastic Storage Modulus of Poly-
Urethane in KPA%
```

```matlab
Edprime=(a22*x.^2)+(a12*x)+a02;    %Elastic Loss Modulus of
Polyurethane in KPA%
Gprime= (b21*x.^2)+(b11*x)+b01;    %Shear Storage Modulus of
Polyurethane in KPA%
Gdprime=(b22*x.^2)+(b12*x)+b02;    %Shear Loss Modulus of Polyurethane
in KPA%
Em=Eprime+Edprime*i;               %Extentional Modulus(Complex) of
Polyurethane in KPA%
Gm=Gprime+Gdprime*i;               %Shear Modulus(Complex) of
Polyurethane in KPA %
vm=(Em)/(2*Gm)-1;                  %Poisson's Ratio(Complex) of
Polyurethane%%
%%%%%%%%%%%%%%%%%%%%%%%%%%%%%%%%%%%%%%%%%%%%%%%%%%%%%%%%%%%%%%%%%%%%%%%%%
%%%%%
%Properties of Carbon Fibers%
Ef  = 230.0e9;
vf = 0.2;
Gf  = Ef/(2*(1+vf));
%%%%%%%%%%%%%%%%%%%%%%%%%%%%%%%%%%%%%%%%%%%%%%%%%%%%%%%%%%%%%%%%%%%%%%%%%
%%%%%
%Properties of Carbon Polyrethane (C/PU) Lamina Only%
%Using Rule of Mixture%
E1=(Ef*Vf)+(Em*Vm);
%In Plane Poisson's Ratio Calculated using Different Models%
%Using Rule of Mixture%
v12=(vf*Vf)+(vm*Vm);
%Transverse Modulus (E2) Calculated Using Different Emperical models%
%Using Halpin-Tsai%
Z= 2;                             %Curve Fitting Parameter%
n = ((Ef./Em)-1)./((Ef./Em)+Z);
E2= Em.*((1+Z*n*Vf)./(1-n*Vf));
%Using Halpin-Tsai%
Z= 2;                             %Curve Fitting Parameter%
n = ((Gf./Gm)-1)./((Gf./Gm)+Z);
G12= Gm.*((1+Z*n*Vf)./(1-n*Vf));
%%%%%%%%%%%%%%%%%%%%%%%%%%%%%%%%%%%%%%%%%%%%%%%%%%%%%%%%%%%%%%%%%%%%%%%%%
%%%%%
%General Material Constants%
nu23    = 0.5;
G13 = G12;
G23 = E2/(2*(1+nu23));
%%%%%%%%%%%%%%%%%%%%%%%%%%%%%%%%%%%%%%%%%%%%%%%%%%%%%%%%%%%%%%%%%%%%%%%%%
%%%%%
%Calculating the Stiffness Matrix [Q] and Complaince Matrix [Sb]%
S11  = 1./E1;
S12  = - v12./E1;
S21  = S12;
S22  = 1./E2;
S33  = 1./G12;
S    = [S11 S12 0; S21 S22 0; 0 0 S33];
Q    = inv(S);
```

```matlab
%%%%%%%%%%%%%%%%%%%%%%%%%%%%%%%%%%%%%%%%%%%%%%%%%%%%%%%%%%%%%%%%%%%%%%%%
%%%%%
% Calculating the Transformation matrices [Sbar] and [Qbar]%
theta = thetd*pi/180;
n     = sin(theta);
m     = cos(theta);
nn    = n*n;
mm    = m*m;
nm    = n*m;
T     = [mm nn 2*nm; nn mm -2*nm; -nm nm mm-nn];
invT  = inv(T);
R     = [1 0 0; 0 1 0; 0 0 2];
invR  = inv(R);
Qbar  = invT*Q*R*T*invR;
Sbar  = inv(Qbar);
%%%%%%%%%%%%%%%%%%%%%%%%%%%%%%%%%%%%%%%%%%%%%%%%%%%%%%%%%%%%%%%%%%%%%%%%
%%%%%
% Calculating the [A], [B] and [D] Matrices%
A = A0 + Qbar*(z(j+1)-z(j));
B = B0 + Qbar*(z(j+1)^2-z(j)^2)/2;
D = D0 + Qbar*(z(j+1)^3-z(j)^3)/3;
A0 = A;
B0 = B;
D0 = D;
end
K = [A B; B D];
C = inv(K);
%%%%%%%%%%%%%%%%%%%%%%%%%%%%%%%%%%%%%%%%%%%%%%%%%%%%%%%%%%%%%%%%%%%%%%%%
%%%%%
% Effective properties of the Laminate%
Ex= 1/(C(1,1)*thickness);     %Effective in-plane x-elastic modulus%
Ey=1/(C(2,2)*thickness);      %Effective in-plane y-elastic modulus%
G=1/(C(3,3)*thickness);       %Effective in-plane shear modulus%
vxy=-(C(1,2)/C(1,1));         %Effective inplane major Poisson's Ratio%
D= 12/thickness^3;
Ebx= D/C(4,4);                %Effective out-of-plane stiffnes(X-
Direction)%
Eby=D/C(4,5);                 %Effective out-of-plane stiffnes(Y-
Direction)%
Gb=D/C(6,6);                  %Effective out-of-plane shear modulus%
Ex_prime= real(Ex);
Ex_dprime= imag(Ex);
Epx(ii) = Ex_prime;
Edpx(ii)= Ex_dprime;
rfrq(ii)= x;
Ey_prime= real(Ey);
Ey_dprime= imag(Ey);
Epy(ii) = Ey_prime;
Edpy(ii)= Ey_dprime;
rfrq(ii)= x;
G_prime= real(G);
G_dprime= imag(G);
```

```matlab
Gp(ii) = G_prime;
Gdp(ii)= G_dprime;
rfrq(ii)= x;
end
% Plot of the Effective Modulus (X-Direction)%
figure
plot(rfrq, Epx,'*')
hold on
plot(rfrq, Edpx, '*')
hold off
grid on
xlabel('Reduced Frequency')
ylabel('Modulus')
legend('Storage modulus','Loss Modulus')
title('Effective Modulus of a Laminate (X-Direction)')
% Plot of the Effective Modulus (Y-Direction)%
figure
plot(rfrq, Epy,'*')
hold on
plot(rfrq, Edpy, '*')
hold off
grid on
xlabel('Reduced Frequency')
ylabel('Modulus')
legend('Storage modulus','Loss Modulus')
title('Effective Modulus of a Laminate (Y-Direction)')
% Plot of the Effective in- plane shear modulus%
figure
plot(rfrq, Gp,'*')
hold on
plot(rfrq, Gdp, '*')
hold off
grid on
xlabel('Reduced Frequency')
ylabel('Modulus')
legend('Storage modulus','Loss Modulus')
title('Effective In-Plane Shear Modulus of a Laminate')
```

A.1.5. Function for generating the damping properties of a three layer laminate

1. At 1Hz of Frequency

```matlab
%%%%TO EVALUATE THE EFFECTIVE DAMPING OF THE 3-LAYER LAMINATE AT 1Hz
FREQUENCy%%%%
close all
clc
clear all
PropertiesofLamina
%Material Properties at !hz and 10Hz%
%Properties of the Lamina at 1Hz%
E1=E1(1,1);
```

```matlab
E2=E2(1,1);
G12=G12(1,1);
%Some assumed data%
v23=0.5;
G13=G12;
G23=E2/(2*(1+v23));
v21=v12*E2/E1;
%Laminate Details%
thickness   = 2.36;  %Thickness of the Laminate%
nl          = 3;     %Number of the layers%
d = thickness/nl;  %Thickness of each layer%
z = [-1.5*d, -0.5*d, 0.5*d, 1.5*d];   %Z-Coordinate vector%
% Constitutive Equation%
Sigx = [1000; 0; 0];  %Uniaxial loading%
Tauxy = [0; 0; 1000]; % Shear loading%
Com = [1000; 0; 1000]; % Combined loading%
%work done per cycle%
W_elast = 0;
W_visco = 0;
theta0 = 0; beta0 = 0;
%Damping for the laminate at 1Hz%
for ii = 1:90
    theta = theta0 + 1*ii;
for jj = 1:90
    beta = beta0 + 1*jj;
    thetav = [theta, beta, theta];
% The global Stiffness and Compliance matrices
A0 = zeros(3);
B0 = zeros(3);
D0= zeros(3);
for j=1:nl
thetad = thetav(j);
Theta=thetad*pi/180;
% Complaince Matrix[S] and Stiffness Matrix[Q] at 1 hz Frequency [S]%
S11  = 1/E1;
S12  = - v12/E1;
S21  = S12;
S22  = 1/E2;
S33  = 1/G12;
S    = [S11 S12 0; S21 S22 0; 0 0 S33];
Q    = inv(S);
n    = sin(Theta);
m    = cos(Theta);
nn   = n*n;
mm   = m*m;
nm   = n*m;
T    = [mm nn 2*nm; nn mm -2*nm; -nm nm mm-nn];
invT = inv(T);
R    = [1 0 0; 0 1 0; 0 0 2];
invR  = inv(R);
%Transformation Matrices for 1hz Frequency%
Qbar    = invT*Q*R*T*invR;
```

```
Sbar   = inv(Qbar);
A = A0 + Qbar*(z(j+1)-z(j));
B=  B0 + Qbar*(z(j+1)^2-z(j)^2)/2;
D = D0 + Qbar*(z(j+1)^3-z(j)^3)/3;
A0 = A;
B0 = B;
D0 = D;
end
K = [A B; B D];    %Stiffness matrix%
C = inv(K);                %Complaince Matrix%
alpha=C(1:3, 1:3);          %Inverse of A matrix%
S_L=alpha*thickness;      %S matrix for the laminate%
Epsxy=S_L*Com;            %The Global Strain Vector%
%To calculate the work done in each layer%
%W=We+Wd*i, W=Work Done, We=Total elastic strain energy, Wd=Total
dissipated energy%
for j=1:nl
thetad=thetav(j);
THeta=thetad*pi/180;
S11  = 1./E1;
S12  = - v12./E1;
S21  = S12;
S22  = 1./E2;
S33  = 1./G12;
S    = [S11 S12 0; S21 S22 0; 0 0 S33];
Q    = inv(S);
n    = sin(THeta);
m    = cos(THeta);
nn   = n*n;
mm   = m*m;
nm   = n*m;
Teps = [mm nn nm; nn mm -nm; -2*nm 2*nm mm-nn]; %Transformation
Matrix%
Eps12=Teps*Epsxy; %Local STrain Vector%
Sig12=Q*Eps12;
W=Sig12.'*Eps12/2;
We(j)=real(W);
Wd(j)=imag(W);
end
if ii ==1 BETA(jj) = beta; end
THETA(ii)  = theta;
Se(jj,ii) = sum(We);
Sd(jj,ii) = sum(Wd);
Eta(jj,ii) = - sum(Wd)/sum(We);
end
end
%Contour Plot%
figure
pcolor(THETA,BETA,Eta)
shading interp
hold on
contour(THETA,BETA,Eta,100,'k')
```
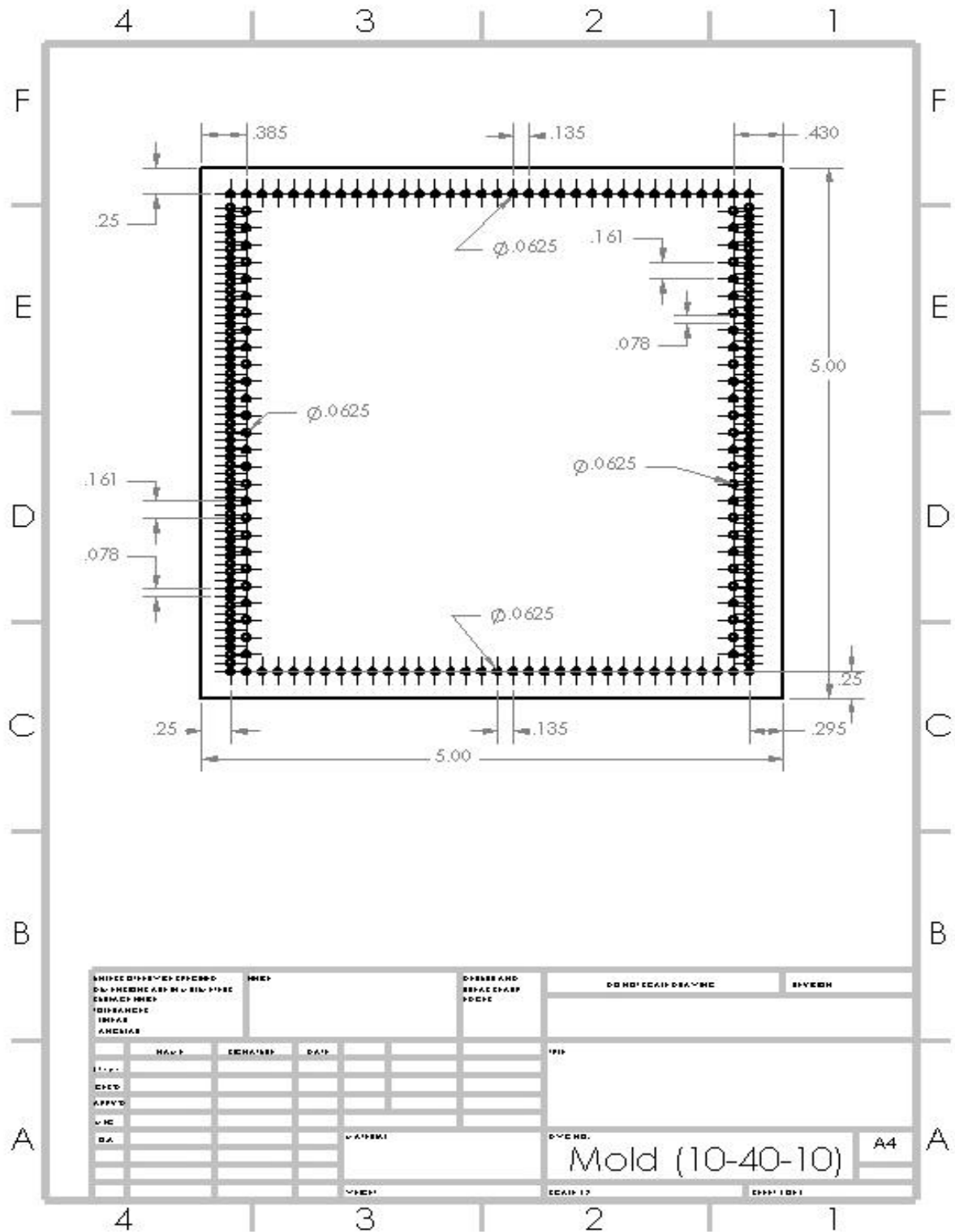
```
title('Contour Plot of Shear Loss Factor(n) @ 1hz ')
xlabel('THETA')
ylabel('BETA')
```

2. At 10Hz of Frequency

```
%%%%TO EVALUATE THE EFFECTIVE DAMPING OF THE 3-LAYER LAMINATE AT 10Hz
FREQUENCY%%%%
close all
clc
clear all
PropertiesofLamina
%Material Properties at !hz and 10Hz%
%Properties of the Lamina at 1Hz%
E1=E1(1,10);
E2=E2(1,10);
G12=G12(1,10);
%Some assumed data%
v23=0.5;
G13=G12;
G23=E2/(2*(1+v23));
v21=v12*E2/E1;
%Laminate Details%
thickness   = 2.36;  %Thickness of the Laminate%
nl          = 3;    %Number of the layers%
d = thickness/nl;  %Thickness of each layer%
z = [-1.5*d, -0.5*d, 0.5*d, 1.5*d];  %Z-Coordinate vector%
% Constitutive Equation%
Sigx = [1000; 0; 0];  %Uniaxial loading%
Tauxy = [0; 0; 1000]; % Shear loading%
Com = [1000; 0; 1000]; % Combined loading%
%work done per cycle%
W_elast = 0;
W_visco = 0;
theta0 = 0; beta0 = 0;
%Damping for the laminate at 1Hz%
for ii = 1:90
    theta = theta0 + 1*ii;
for jj = 1:90
    beta = beta0 + 1*jj;
    thetav = [theta, beta, theta];
% The global Stiffness and Compliance matrices
A0 = zeros(3);
B0 = zeros(3);
D0= zeros(3);
for j=1:nl
thetad = thetav(j);
Theta=thetad*pi/180;
% Complaince Matrix[S] and Stiffness Matrix[Q] at 1 hz Frequency [S]%
S11  = 1/E1;
S12  = - v12/E1;
S21  = S12;
S22  = 1/E2;
```

```
S33   = 1/G12;
S     = [S11 S12 0; S21 S22 0; 0 0 S33];
Q     = inv(S);
n     = sin(Theta);
m     = cos(Theta);
nn    = n*n;
mm    = m*m;
nm    = n*m;
T     = [mm nn 2*nm; nn mm -2*nm; -nm nm mm-nn];
invT  = inv(T);
R     = [1 0 0; 0 1 0; 0 0 2];
invR  = inv(R);
%Transformation Matrices for 1hz Frequency%
Qbar    = invT*Q*R*T*invR;
Sbar    = inv(Qbar);
A = A0 + Qbar*(z(j+1)-z(j));
B=  B0 + Qbar*(z(j+1)^2-z(j)^2)/2;
D = D0 + Qbar*(z(j+1)^3-z(j)^3)/3;
A0 = A;
B0 = B;
D0 = D;
end
K = [A B; B D];    %Stiffness matrix%
C = inv(K);                %Complaince Matrix%
alpha=C(1:3, 1:3);        %Inverse of A matrix%
S_L=alpha*thickness;      %S matrix for the laminate%
Epsxy=S_L*Sigx;           %The Global Strain Vector%
%To calculate the work done in each layer%
%W=We+Wd*i, W=Work Done, We=Total elastic strain energy, Wd=Total
dissipated energy%
for j=1:nl
thetad=thetav(j);
THeta=thetad*pi/180;
S11   = 1./E1;
S12   = - v12./E1;
S21   = S12;
S22   = 1./E2;
S33   = 1./G12;
S     = [S11 S12 0; S21 S22 0; 0 0 S33];
Q     = inv(S);
n     = sin(THeta);
m     = cos(THeta);
nn    = n*n;
mm    = m*m;
nm    = n*m;
Teps = [mm nn nm; nn mm -nm; -2*nm 2*nm mm-nn]; %Transformation
Matrix%
Eps12=Teps*Epsxy; %Local STrain Vector%
Sig12=Q*Eps12;
W=Sig12.'*Eps12/2;
We(j)=real(W);
Wd(j)=imag(W);
```

```
end
if ii ==1 BETA(jj) = beta; end
THETA(ii)  = theta;
Se(jj,ii) = sum(We);
Sd(jj,ii) = sum(Wd);
Eta(jj,ii) = - sum(Wd)/sum(We);
end
end
%Contour Plot%
figure
pcolor(THETA,BETA,Eta)
shading interp
hold on
contour(THETA,BETA,Eta,100,'k')
title('Contour Plot of Shear Loss Factor(n) @ 10hz ')
xlabel('THETA')
ylabel('BETA')
```
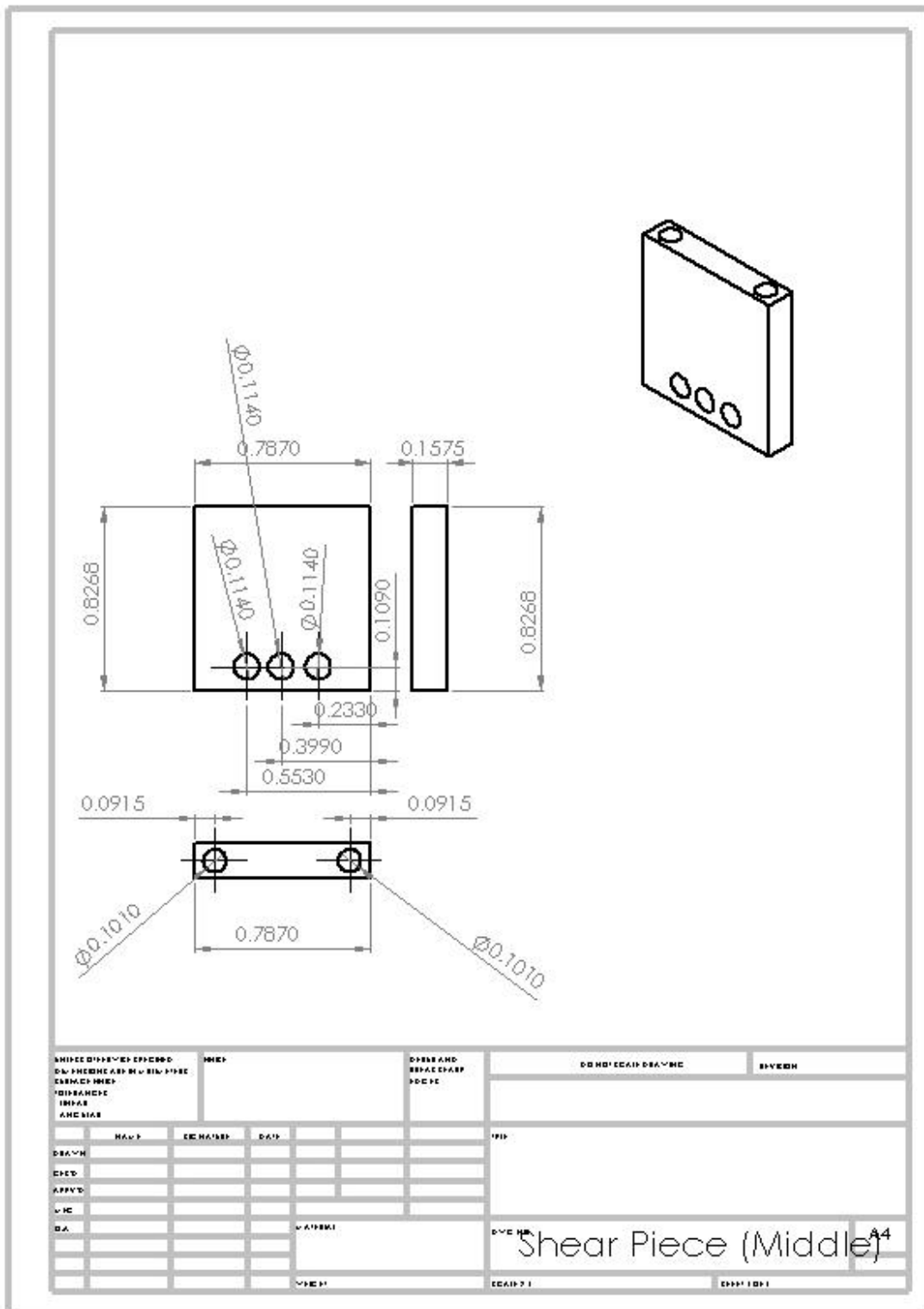
Appendix B
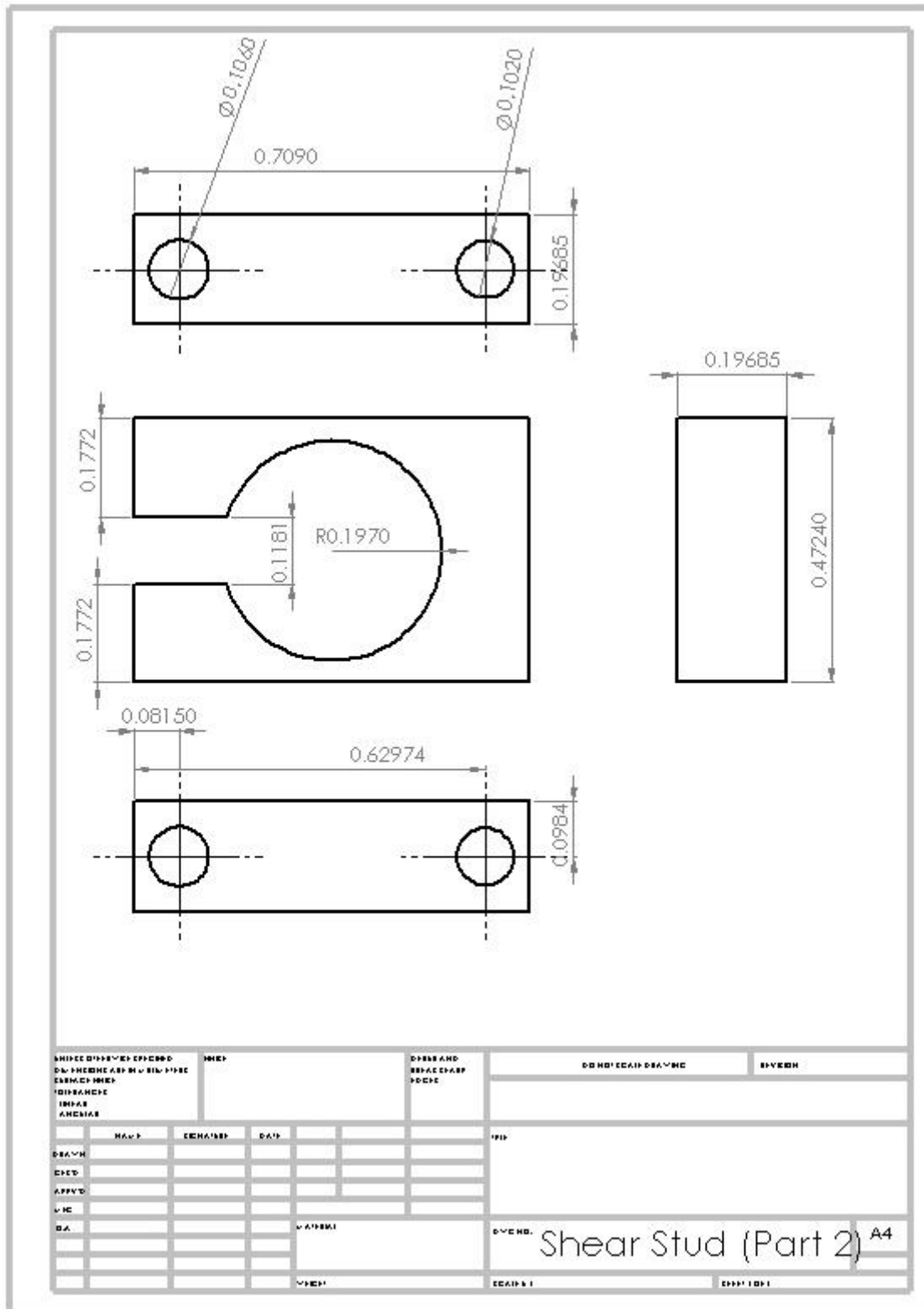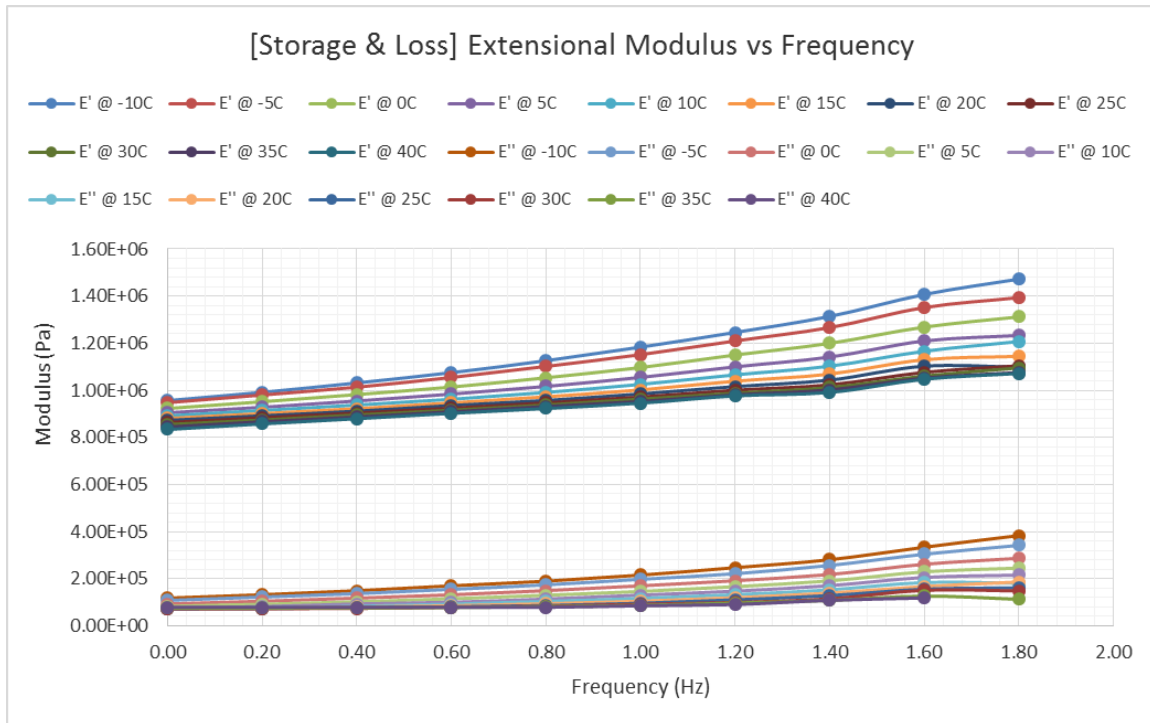## Drawing of the Open Mold for Laminate (10/40/10):-

Drawing of the Open Mold for Lamina:-

Drawing of the Shear Fixtures:-

Shear Piece (Middle)

Ø0.3940

Ø0.2380

0.2380

0.3940

0.1560

Shear Stud (Cylinder)

1.3000
0.9850
0.4370
0.12
0.55
0.09843
R0.0530
Ø0.1060
Ø0.1060
Ø0.1060
0.20

0.19685
0.1060
0.19685
0.19685
1.41732

Shear Stud (Part 1)

Appendix C
Sample Plots of the Raw Data from the DMA
Extensional Moduli of Polyurethane (PU)

(a) Plot of the Extensional(Storage and Loss) Moduli for Polyurethane

[Storage & Loss] Extensional Modulus vs Frequency

(b) Plot of the Loss Tangent (Tan(δ)) values for Extensional Moduli

Loss Tangent [Tan (D)] vs Frequency

Shear Moduli of Polyurethane (PU)

(a) Plot of the Shear (Storage and Loss) Moduli for Polyurethane

(b) Plot of the Loss Tangent (Tan(δ)) values for Shear Moduli

Transverse Moduli of a Carbon/Polyurethane (C/PU) Lamina

(a) Extensional Transverse (Storage and Loss) Moduli

(b) Plot of Loss Tangent Values for Transverse Moduli

In-Plane Shear Moduli of a Carbon/Polyurethane (C/PU) Lamina
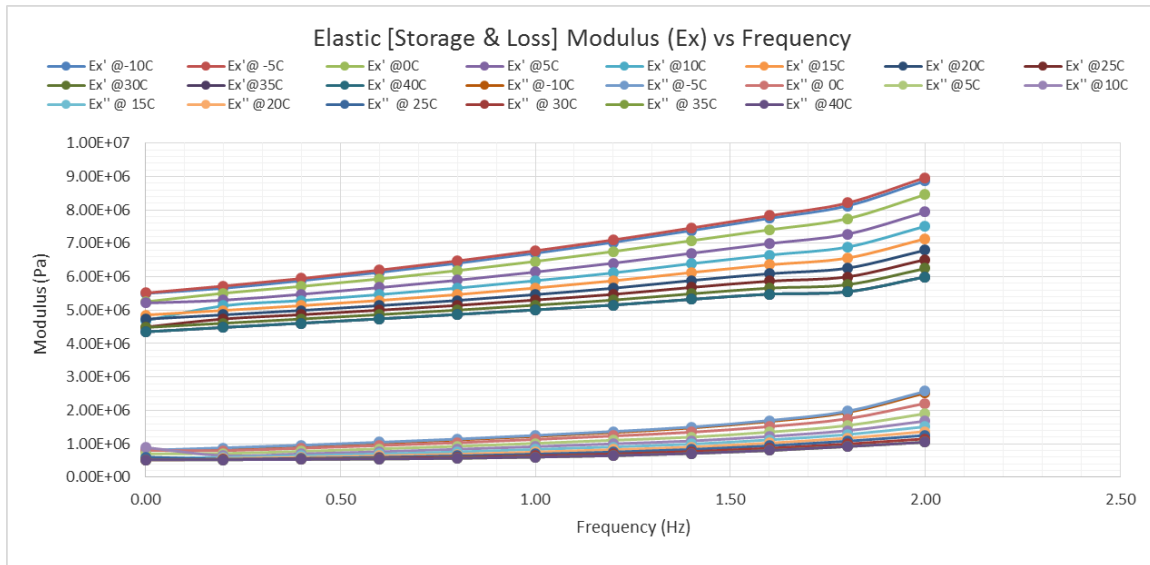
(a) In-Plane Shear (Storage and Loss) Moduli

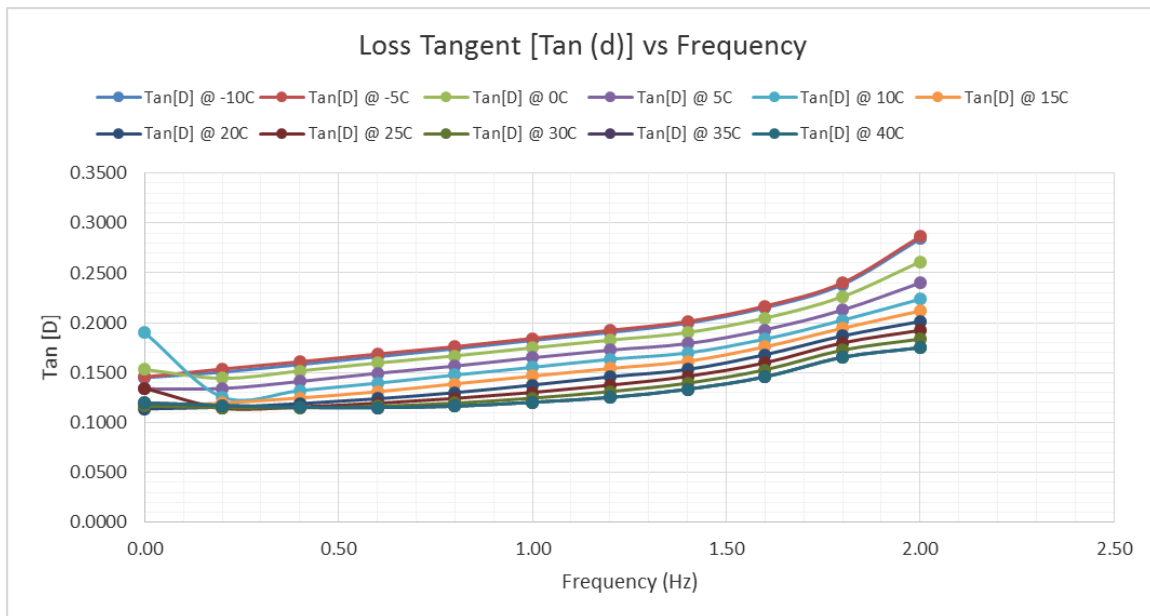**(b) Plot of Loss Tangent Values for In-Plane Shear Moduli**

Elastic Moduli (E$_x$) of a Carbon/Polyurethane (C/PU) Laminate
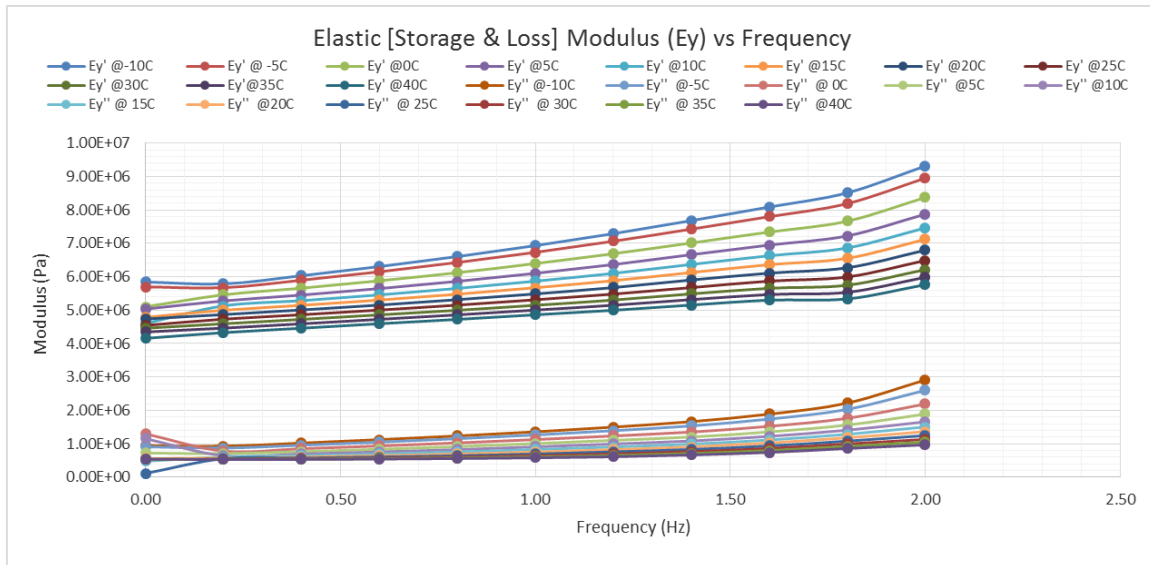
(a) Elastic (Storage and Loss) Moduli (E$_x$)

Elastic [Storage & Loss] Modulus (Ex) vs Frequency

(b) Plot of Loss Tangent Values for Laminate Extensional Moduli (E$_x$)
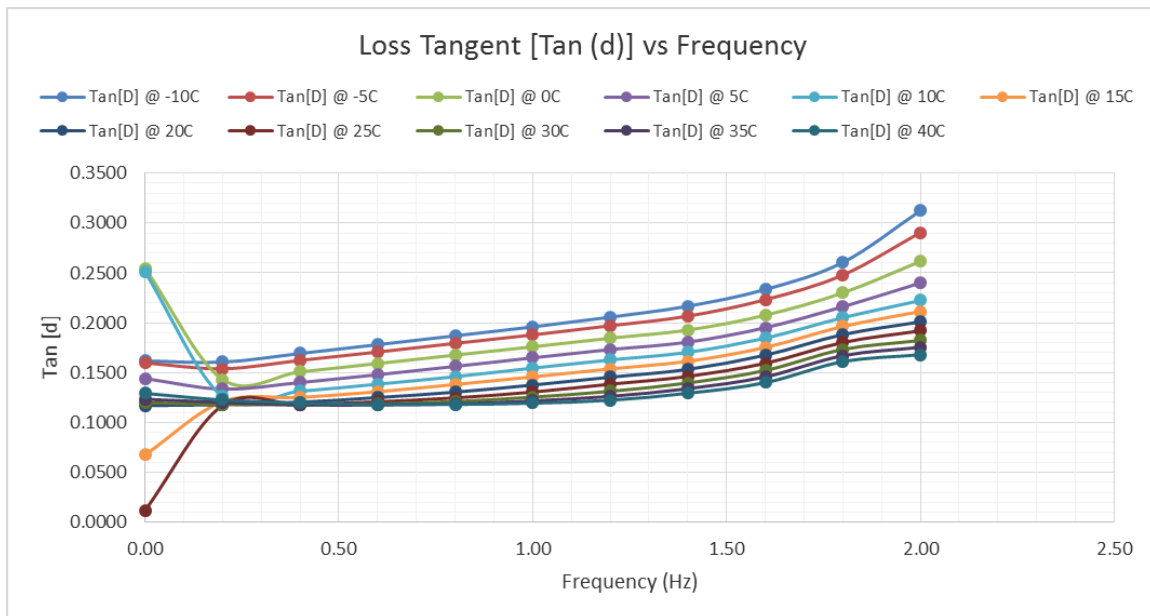

Loss Tangent [Tan (d)] vs Frequency

Elastic Moduli (E_y) of a Carbon/Polyurethane (C/PU) Laminate

(c) Elastic (Storage and Loss) Moduli (E_y)
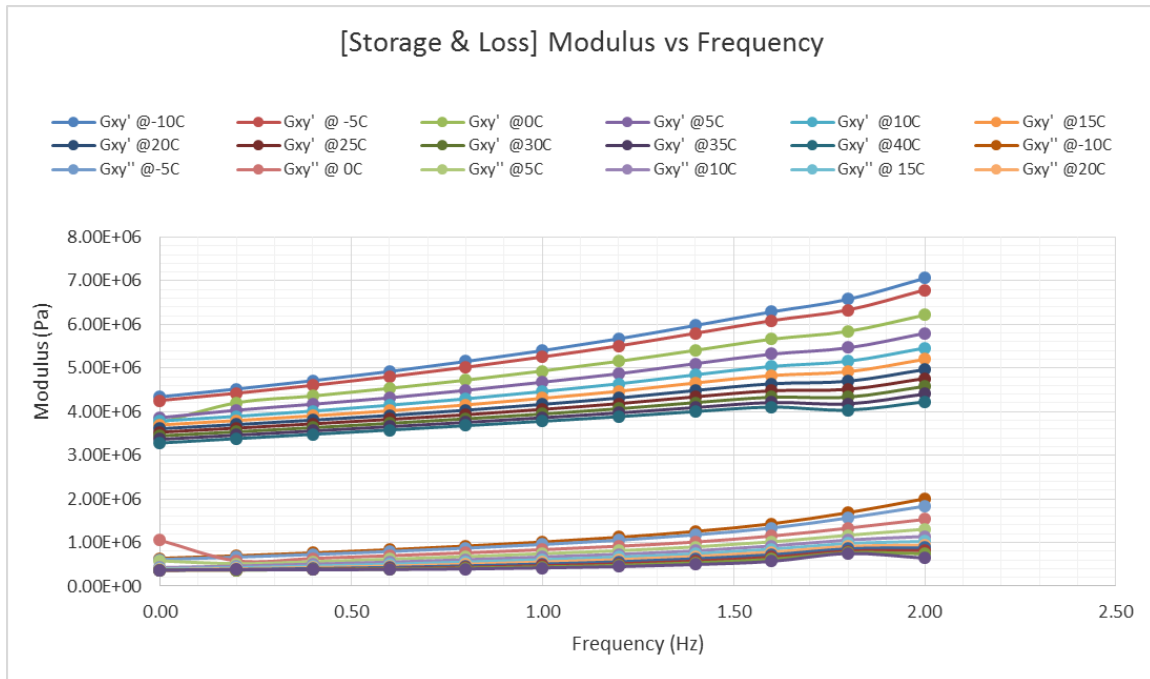

(d) Plot of Loss Tangent Values for Laminate Extensional Moduli (E_y)

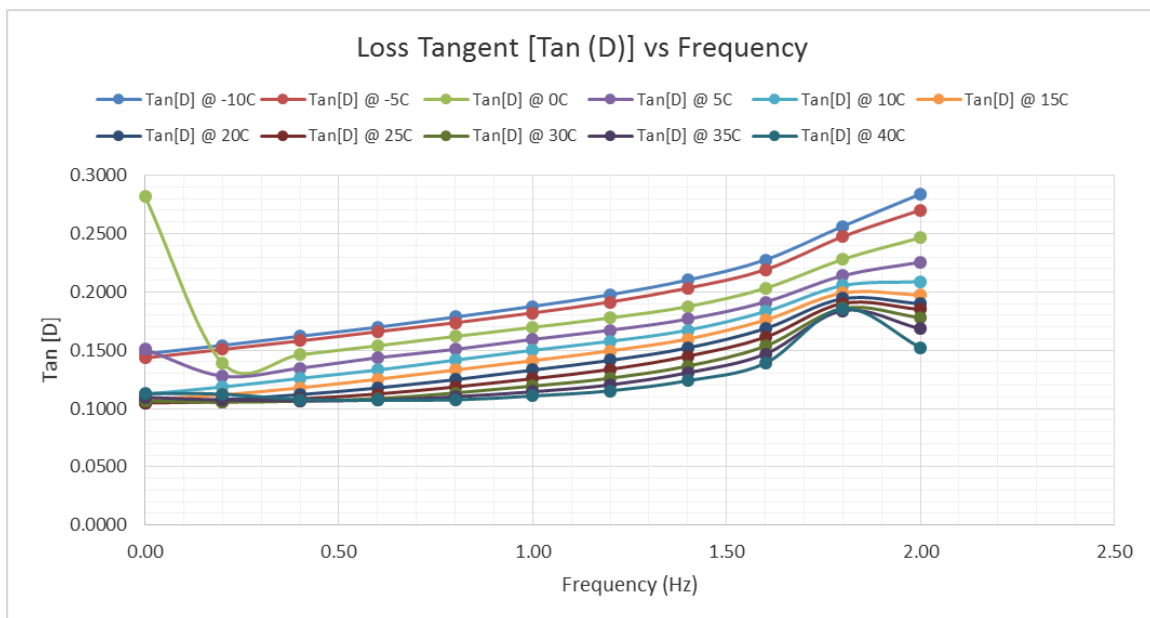# Shear Moduli (G$_{xy}$) of a Carbon/Polyurethane (C/PU) Laminate
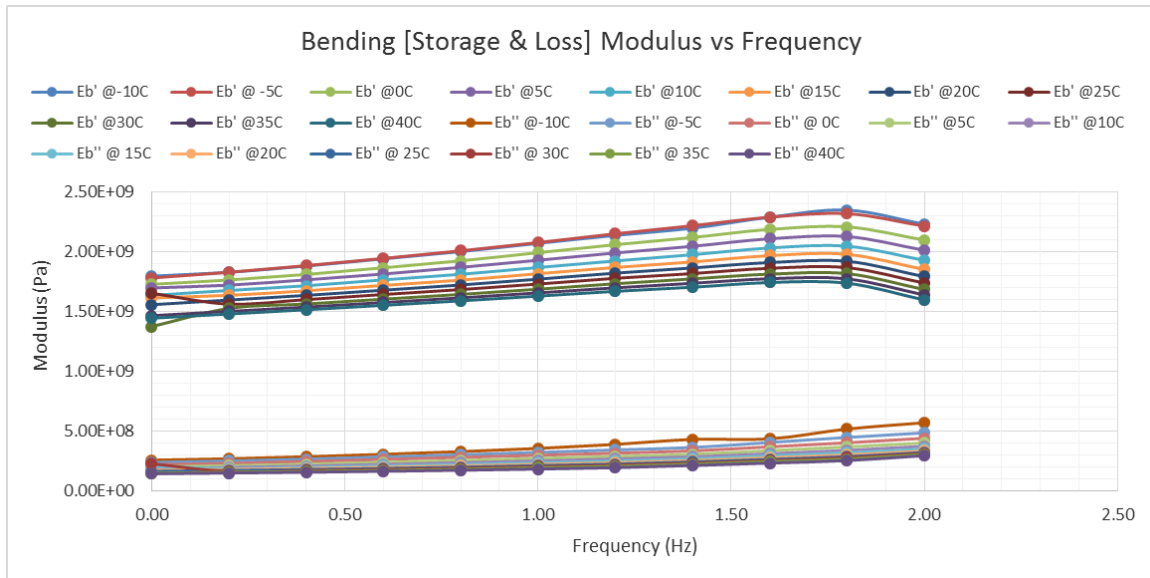
(a) Shear (Storage and Loss) Moduli (G$_{xy}$)

(b) Plot of Loss Tangent Values for Laminate Extensional Moduli (G$_{xy}$)

Bending Moduli (E$_b$) of a Carbon/Polyurethane (C/PU) Laminate

(a) Bending (Storage and Loss) Moduli (E$_b$)

Bending [Storage & Loss] Modulus vs Frequency

(b) Plot of Loss Tangent Values for Laminate Extensional Moduli (E$_b$)

Loss Tangent [Tan (D)] vs Frequency